

174

0-315-12488-1



National Library of Canada

Bibliothèque nationale du Canada

Canadian Theses Division

Division des thèses canadiennes

Ottawa, Canada
K1A 0N4

60399

PERMISSION TO MICROFILM — AUTORISATION DE MICROFILMER

• Please print or type — Écrire en lettres moulées ou dactylographier

Full Name of Author — Nom complet de l'auteur

PAUL ANTHONY WAGNER

Date of Birth — Date de naissance

21 July, 1955

Country of Birth — Lieu de naissance

U.S.A.

Permanent Address — Résidence fixe

O1B, 9012 112 St
EDMONTON, ALBERTA T6G 2C5

Title of Thesis — Titre de la thèse

GEOCHRONOLOGY OF THE AMERALIK DYKES AT
ISUA, WEST GREENLAND

University — Université

UNIVERSITY OF ALBERTA

Degree for which thesis was presented — Grade pour lequel cette thèse fut présentée

Master of Science

Year this degree conferred — Année d'obtention de ce grade

1982

Name of Supervisor — Nom du directeur de thèse

Dr. Halfdan Baadsgaard

Permission is hereby granted to the NATIONAL LIBRARY OF CANADA to microfilm this thesis and to lend or sell copies of the film.

L'autorisation est, par la présente, accordée à la BIBLIOTHÈQUE NATIONALE DU CANADA de microfilmer cette thèse et de prêter ou de vendre des exemplaires du film.

The author reserves other publication rights, and neither the thesis nor extensive extracts from it may be printed or otherwise reproduced without the author's written permission.

L'auteur se réserve les autres droits de publication; ni la thèse ni de longs extraits de celle-ci ne doivent être imprimés ou autrement reproduits sans l'autorisation écrite de l'auteur.

Date

13 October 1982

Signature

Paul Anthony Wagner

CANADIAN THESES ON MICROFICHE

I.S.B.N.

THESES CANADIENNES SUR MICROFICHE



National Library of Canada
Collections Development Branch

Canadian Theses on
Microfiche Service

Ottawa, Canada
K1A 0N4

Bibliothèque nationale du Canada
Direction du développement des collections

Service des thèses canadiennes
sur microfiche

NOTICE

The quality of this microfiche is heavily dependent upon the quality of the original thesis submitted for microfilming. Every effort has been made to ensure the highest quality of reproduction possible.

If pages are missing, contact the university which granted the degree.

Some pages may have indistinct print especially if the original pages were typed with a poor typewriter ribbon or if the university sent us a poor photocopy.

Previously copyrighted materials (journal articles, published tests, etc.) are not filmed.

Reproduction in full or in part of this film is governed by the Canadian Copyright Act, R.S.C. 1970, c. C-30. Please read the authorization forms which accompany this thesis.

THIS DISSERTATION
HAS BEEN MICROFILMED
EXACTLY AS RECEIVED

AVIS

La qualité de cette microfiche dépend grandement de la qualité de la thèse soumise au microfilmage. Nous avons tout fait pour assurer une qualité supérieure de reproduction.

S'il manque des pages, veuillez communiquer avec l'université qui a conféré le grade.

La qualité d'impression de certaines pages peut laisser à désirer, surtout si les pages originales ont été dactylographiées à l'aide d'un ruban usé ou si l'université nous a fait parvenir une photocopie de mauvaise qualité.

Les documents qui font déjà l'objet d'un droit d'auteur (articles de revue, examens publiés, etc.) ne sont pas microfilmés.

La reproduction, même partielle, de ce microfilm est soumise à la Loi canadienne sur le droit d'auteur, SRC 1970, c. C-30. Veuillez prendre connaissance des formules d'autorisation qui accompagnent cette thèse.

LA THÈSE A ÉTÉ
MICROFILMÉE TELLÉ QUE
NOUS L'AVONS REÇUE

THE UNIVERSITY OF ALBERTA

"Geochronology of the Ameralik Dykes at Isua, West Greenland"

by



Paul Anthony Wagner

A THESIS

SUBMITTED TO THE FACULTY OF GRADUATE STUDIES AND RESEARCH

IN PARTIAL FULFILMENT OF THE REQUIREMENTS FOR THE DEGREE

OF Master of Science

Department of Geology

EDMONTON, ALBERTA

Fall, 1982

THE UNIVERSITY OF ALBERTA
RELEASE FORM

NAME OF AUTHOR Paul Anthony Wagner
TITLE OF THESIS "Geochronology of the Ameralik Dykes at Isua, West
Greenland"
DEGREE FOR WHICH THESIS WAS PRESENTED Master of Science
YEAR THIS DEGREE GRANTED Fall, 1982

Permission is hereby granted to THE UNIVERSITY OF ALBERTA LIBRARY to reproduce single copies of this thesis and to lend or sell such copies for private, scholarly or scientific research purposes only.

The author reserves other publication rights, and neither the thesis nor extensive extracts from it may be printed or otherwise reproduced without the author's written permission.

(SIGNED)

Paul Anthony Wagner

PERMANENT ADDRESS:

*018 2012 112 Street
Edmonton, Alberta, T6G 2G5
Canada*

DATED *08 October* 1982

THE UNIVERSITY OF ALBERTA

FACULTY OF GRADUATE STUDIES AND RESEARCH

The undersigned certify that they have read, and recommend to the Faculty of Graduate Studies and Research, for acceptance, a thesis entitled "Geochronology of the Ameralik Dykes at Isua, West Greenland" submitted by Paul Anthony Wagner in partial fulfilment of the requirements for the degree of Master of Science.

A. Boelsgaard

Supervisor

Gh. Cumming

R. A. Brinich

R. S. J. Lambert

Date *8 Oct 82*

Dedication

This thesis is dedicated
to the memory of Paul Bains and Gerry Groves,
from whom we learned so much about ourselves,
and who shall live in our memories for many long years.

ABSTRACT

Whole rock samples of the early Proterozoic Archaean Ameralik dykes from Isua, West Greenland have been analyzed for their Rb-Sr and Pb-Pb isotopic compositions. Pb-Pb whole rock data obtained on analyses from two dykes indicate emplacement occurred $3,197 \pm 45$ Ma ago, based on growth curve intercept ages of $3,192 \pm 53$ Ma and $3,209 \pm 77$ Ma obtained for the dykes, collected more than 5 km. apart, hosted by different country rocks. It is suggested that the isotopic compositions represent a two component mixture of leads from both the primary basaltic magma and extracted from the host rocks through partial anatexis during emplacement. Rb-Sr data are inconclusive in confirmation of the age of emplacement. The widespread scatter in the data suggests deuteritic alteration, migration of alkalis, later (Proterozoic) metamorphism and contamination of the primary magma by assimilation of older crust. The data are consistent with models of primary magma contamination masking original isotopic compositions.

Rb-Sr and Pb isotopic analysis of samples of a "Proterozoic" Isua dyke indicated geochemical characteristics and isotopic variability. This dyke was apparently not subjected to similar degrees of alteration and metamorphism found in the Ameralik dykes. Mineralogical and strontium data suggest open system chemical behaviour during and after emplacement. Pb data yields an "anomalous" growth curve intercept age of $3,233 \pm 131$ Ma, suggesting this particular dyke has digested sizeable quantities of older crustal material during emplacement.

ACKNOWLEDGEMENTS

I would like to express my sincere gratitude to Dr. H. Baadsgaard for the time and patience he gave in introducing me to the theory and methods of isotope geology. His encouragement, comments and continual support during the many memorable and frustrating moments encountered during the course of this study are deeply appreciated. Mass spectrometric facilities used were meticulously cared for by Dr. S.L. Cumming and Mr. H. McCullough. To Dragan Krstic, who has helped in so many ways, a simple thank you seems insignificant. I am indebted to L. Wayne Day for his help in sample preparation, analyses and partial loan of his laboratory facilities. Dr. J.R. Richards is thanked for his critical review of the manuscript.

Dr. H. Baadsgaard, Dr. R.C.O. Gill and Dr. A. Nutman are thanked for trudging through the summer snows of Greenland in the collection of samples for this project. I am fortunate in having many people with whom I was able to have fruitful and informative discussions, but those held with Drs. D. Bridgwater and V. McGregor stand foremost.

I would like to take this opportunity to especially thank my family for their support, encouragement and understanding given during the course of this study.

Financial support during this study was given by the Department of Geology in the form of Graduate Teaching Assistantships and University of Alberta bursaries.

Table of Contents

Chapter	Page
I. INTRODUCTION	1
II. GEOLOGY OF THE ISUA AREA	3
A. General Geology	3
Geochronology	6
B. Geology at Isua	6
Isua Supracrustals	6
Amitsoq Gneiss	8
Ameralik Dykes	10
III. SAMPLING AND PETROGRAPHIC DESCRIPTIONS OF ISUA DYKES	12
A. Introduction	12
B. Mineralogy and Petrology	12
Dyke I	14
Dyke II	17
Dyke III	23
Random Samples	25
C. Summary	25
IV. ANALYTICAL	27
Rb/Sr	27
Pb/Pb	28
V. RESULTS AND DISCUSSION	29
A. Ameralik Dykes, Rubidium-Strontium Results	29
B. Ameralik Dykes, Lead-Lead Results	38
C. Proterozoic Dyke III, Rubidium-Strontium and Lead-Lead results	46
VI. INTERPRETATION AND CONCLUSIONS	51
A. Interpretation of the Results	51
B. Conclusions	58
VII. REFERENCES CITED	61
VIII. APPENDIX I	66

IX. APPENDIX II	76
A. Rb-Sr Analytical Procedures	76
B. Pb-Pb Analytical Procedures	78

LIST OF FIGURES

Figure 1: Location of the Godthaabsfjord-Isua area	4
Figure 2: General geology of the Isua area	7
Figure 3: Sample locations	13
Figure 4: Sample locations; Dyke II	18
Figure 5: Sample locations; Dyke III	24
Figure 6: Plot of $^{87}\text{Sr}/^{86}\text{Sr}$ versus $^{87}\text{Rb}/^{86}\text{Sr}$ ratios for whole rock Ameralik Dyke analyses	30
Figure 7: Plot of $^{87}\text{Sr}/^{86}\text{Sr}$ versus $^{87}\text{Rb}/^{86}\text{Sr}$ ratios for Dyke I	31
Figure 8: Plot of $^{87}\text{Sr}/^{86}\text{Sr}$ versus $^{87}\text{Rb}/^{86}\text{Sr}$ ratios for Dyke II	32
Figure 9: Sr concentrations in traverses across Dyke I	33
Figure 10: Sr concentrations in traverses across Dyke II	34
Figure 11: Rb concentrations in traverses across Dyke I	36
Figure 12: Rb concentrations in traverses across Dyke II	37
Figure 13: Plot of $^{207}\text{Pb}/^{204}\text{Pb}$ versus $^{206}\text{Pb}/^{204}\text{Pb}$ for whole rock Ameralik Dyke samples	39

Figure 14: Plot of $^{207}\text{Pb}/^{206}\text{Pb}$ ratios for Dykes I and II	41
Figure 15: Plot of $^{207}\text{Pb}/^{204}\text{Pb}$ versus $^{206}\text{Pb}/^{204}\text{Pb}$ for Dyke I	43
Figure 16: Plot of $^{207}\text{Pb}/^{204}\text{Pb}$ versus $^{206}\text{Pb}/^{204}\text{Pb}$ for Dyke II	45
Figure 17: Plot of $^{87}\text{Sr}/^{86}\text{Sr}$ versus $^{87}\text{Rb}/^{86}\text{Sr}$ ratios for the Proterozoic Dyke	47
Figure 18: Plot of $^{207}\text{Pb}/^{204}\text{Pb}$ versus $^{206}\text{Pb}/^{204}\text{Pb}$ ratios for the Proterozoic Dyke	48
Figure 19: Variations in Rb, Sr and $^{207}\text{Pb}/^{206}\text{Pb}$ in traverses across the Proterozoic Dyke	49
Figure 20: Plot of $^{207}\text{Pb}/^{204}\text{Pb}$ versus $^{206}\text{Pb}/^{204}\text{Pb}$ for whole rock Amealik Dykes showing assimilation of older, less radiogenic lead	56

LIST OF PLATES

Plate 1: Dyke I; Recrystallized hornblende and feldspar with scapolite and clinozoisite, x40, plane polarized light	15
Plate 2: Dyke I; Recrystallized hornblende and feldspar with scapolite and clinozoisite, x40, crossed nicols	15
Plate 3: Dyke I; Recrystallized hornblende with clinozoisite/epidote clot, no evidence of feldspar, x40, plane polarized light	16
Plate 4: Dyke I; Recrystallized hornblende with clinozoisite/epidote clot, no evidence of feldspar, x40, crossed nicols	16
Plate 5: Dyke II; Clinopyroxene altering to hornblende, slight uraltic alteration of the clinopyroxenes is also visible, x40, plane polarized light	19
Plate 6: Dyke II; Olivine altering to serpentine group minerals (antigorite-lizardite?), enclosed in clinopyroxene, x40, plane polarized light	19
Plate 7: Dyke II; Ilmenite-magnetite altering to sphene in turn to biotite, x40, plane polarized light	20
Plate 8: Dyke II; Development of uraltic and alkali alteration in clinopyroxene and amphibole, x40, plane polarized light	20
Plate 9: Dyke II; Development of uraltic and alkali alteration in clinopyroxene and amphibole, x40, crossed nicols	21

Plate 10: Dyke III; Primary micropegmatite, zoned plagioclase and clinopyroxene,

x40, crossed nicols

2

LIST OF TABLES

Table 1: General geologic history of the Godthaabsfjord-Isua area

Table 2: Rb/Sr Isotope Results, Isua Dykes

Table 3: Corrected Pb/Pb Isotope Results, Isua Dykes

Table 4: Rb/Sr Isotope Data, Isua Proterozoic Dyke

Table 5: Corrected Pb/Pb Isotope Results, Isua Proterozoic Dyke

I. INTRODUCTION

Dyke swarms are useful in the investigation of igneous terranes in that they represent short-lived magmatic events. These short-lived events provide a record in geologic time, of a moment which is preserved and can be later studied. Emplacement and subsequent geological processes may, however, initiate changes within the parent magma or crystallized rock which obscure concise interpretations. This is especially true in the study of very old dykes.

During 1968, small bodies of homogeneous, fine to medium grained black amphibolite were described as abundant inclusions in the gneisses around Godthaab and the coast of the outer part of Ameralik. The inclusions had been deformed, broken up and migmatized by granite veins. Where undeformed, the amphibolites took on the appearance of dykes and were noted to be discordant to the country rocks. These amphibolite bodies were later named Ameralik after their place of original discovery (McGregor, 1968).

With continued mapping in the Godthaabsfjord area, it was apparent that many lithological units present were intercalated, some of which contained abundant Ameralik inclusions, others, none at all. The units which contain abundant Ameralik fragments are composed of quartzo-feldspathic gneisses and enclaves of more basic material, named the Amitsoq gneiss and the Isua supracrustals.

The lithological units in and around Godthaab which do not contain any Ameralik inclusions include a second major quartzo-feldspathic gneiss, the Nuk gneiss, another meta-basic unit, the Malene supracrustals and thick sheets of very calcic meta-anorthosite, the Fiskenaesset anorthosite complex. The Nuk gneisses are known to intrude and migmatize the Amitsoq gneiss, the Malene supracrustals and the Fiskenaesset complex.

The nature of the intrusive relationship between the Ameralik dykes, the Amitsoq and Nuk gneisses aid in the stratigraphic interpretation of the Godthaabsfjord area. Prior to isotope studies of the gneissic complexes, the sole criteria identifying the separate orthogneisses was the presence or the absence of Ameralik dyke inclusions. Subsequent

studies (Black *et al.*, 1971, 1973; Baadsgaard, 1973, 1976; Baadsgaard and McGregor, 1980; Moorbath *et al.*, 1972, 1973) have shown the age of the Amitsoq gneisses to be approximately 3,700 Ma and 3,050 Ma for the Nuk gneisses. To date, there has been no successful direct measurement of the exact age of the Ameralik dykes. The only constraints placed upon their age are those outlined by the ages of the rocks they intrude and the rocks they do not intrude.

The primary purpose of this study was to establish the age of emplacement of the Ameralik dykes and examine any pre or post emplacement geological alteration which may have occurred.

Initial sampling was done on a random basis assuming isotopic homogeneity between individual dykes. The preliminary isotope results indicated widespread heterogeneous behaviour of the isotopes concerned, and possible inhomogeneity within individual dykes. Subsequent collections were made on a twofold premise; to investigate the original goal of this study and to examine pre and post emplacement effects which may have altered the isotope systematics of the dykes. An effort was made to avoid collection of samples which showed any signs of metamorphic alteration, strain, veining or intense weathering.

It was also apparent that other problems unique to early Archaean rocks would also have to be dealt with, such as high crustal level of emplacement into possibly still warm country rocks, higher heat flux present in the thin Archaean crust and uncertainties pertaining to possible tectonism active during the Archaean. Also to be examined was the possibility of assimilation of pre-existing crustal material during emplacement of the dykes. In order to examine all the possible combinations which might alter the isotopic composition of the rocks in any manner, a carefully defined collection program was established. Samples would be taken across and along various dykes hosted by the two major lithologic units as a control for examining the parameters detailed above.

II. GEOLOGY OF THE ISUA AREA

A. General Geology

The Archaean gneiss complex of Greenland (Figure 1), extending from Itivdleq to Ivigtut on the west coast and from Gyldenloves Fjord to Mogens Heinesen Fjord on the east coast, has remained unaffected by major geologic events from 2,600 Ma to the present (Bridgwater *et al.*, 1974, 1976; Myers, 1976). It is bounded to the north and the south by similar rocks of the Nagssugtoqidian and Ketilidian mobile belts, both extensively reworked during the Proterozoic (Allaart, 1976a; Escher *et al.*, 1976; Myers, 1976).

Approximately 75 percent of the complex is covered by the inland ice sheet; only sections nearer the coast are ice free. Of the rock exposed, 80 to 90 percent consists of granitoid quartzo-felspathic gneiss, apparently derived from acid to intermediate igneous rocks (McGregor, 1973; Bridgwater *et al.*, 1974; Nutman *et al.*, 1982). These in turn are intercalated with units of amphibolite, derived predominantly from metavolcanics and a minor paragneiss component (Bridgwater and McGregor, 1974; Bridgwater *et al.*, 1976; Allaart, 1976a, b; McGregor and Mason, 1977).

The amphibolites display a layered nature. Subunits may vary in thickness from several centimetres to several kilometres (Bridgwater *et al.*, 1976). The layered nature of the rock is attributed to large scale injection of sheet-like igneous rocks, coupled with intense deformation of the entire package, at which time it is believed interleaving and folding of rocks of widespread provenance and lithologies occurred (Bridgwater *et al.*, 1974; McGregor, 1979).

Most of the rocks in the complex are characterized by mineral assemblages commonly representing amphibolite to granulite facies metamorphism which occurred at depths of 25 to 35 kilometres (Wells, 1976; Boak and Dymek, 1982). The present level of exposure presents a moderately deep section of the Archaean crust (McGregor, 1979), locally preserving inclusions of pre-existing crustal material. The best exposures of both ancient supracrustal rocks and gneisses are found at Isua, approximately 150 km north-east of Godthaab (Figure 1).

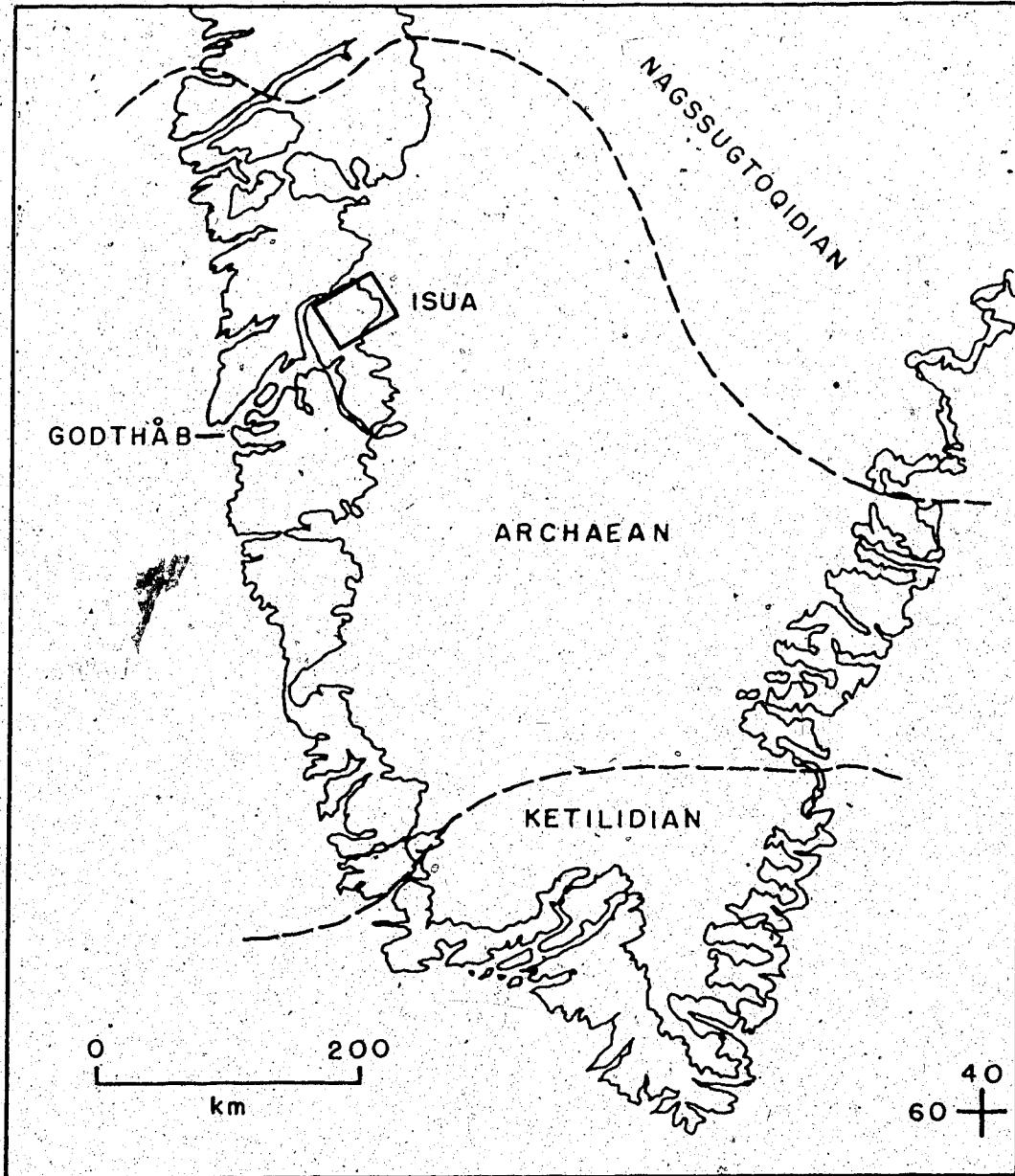


Figure 1: Location of the Godthaabsfjord-Isua area, the Archaean craton, the Nagssugtoquidian and Ketilidian mobile belts to the north and south.

Table 1. Simplified table of events from the Archaean of Greenland¹

<u>Geological Event</u>	<u>Time</u>
1) Deposition of the Isua supracrustals. Basic and ultrabasic lavas and intrusions, basic tuffs, quartzites, siltstones, pelites, ironstones and calcareous rocks. Acid volcanic fragments in a conglomerate.	>3,750 Ma.
2) Intrusion of syntectonic and late tectonic granites (parents of the Amitsoq gneisses) possibly contemporaneous with upper acid volcanic part of the Isua supracrustals.	ca. 3,750 Ma
3) Deformation and metamorphism of the Isua supracrustals and the Amitsoq gneisses.	
4) Intrusion of abundant swarms of basic dykes (Ameralik dykes) during regional stress.	
5) Extrusion of basic and intermediate volcanics, intrusion of ultrabasic bodies and layered basic igneous bodies, deposition of sediments including pelites, aluminous quartzites and minor calcareous units (Malene supracrustals).	3,040 Ma.
6) Intrusion of major suites of syntectonic and late tectonic calc-alkaline rocks as subconcordant sheets (Nuk gneisses).	3,040 Ma.
7) Intense deformation with formation of major nappes, followed by less intense deformation, producing upright folds.	to 2,800 Ma.
8) Emplacement of potash granites associated with NE-SW flexures in the Godthaabsfjord area (Qorqut granite). Widespread post-tectonic pegmatite swarms.	2,600 Ma.
9) Emplacement of at least three regional swarms of basic dykes, transcurrent movement along NE and SW faults. Plutonic activity in area to north and south of craton.	to 1,750 Ma.
10) Slight local metamorphism throughout Archaean block.	ca. 1,600 Ma.

¹After Bridgwater et al., 1976, p.22.

Geochronology

Numerous geologic and isotopic studies in the Isua area (McGregor, 1968, 1969, 1973; Black *et al.*, 1971, 1973; Baadsgaard, 1973, 1976; Moorbath *et al.*, 1972, 1973, 1975, 1977; Pankhurst *et al.*, 1973a, b; Bridgwater and McGregor, 1974a, b; Baadsgaard *et al.*, 1976) have delineated the presence of six major lithostratigraphic and chronostratigraphic units ranging in age from >3,750 Ma to 2,600 Ma. Table 1 lists the major geologic and tectonic events recorded in the Godthaabsfjord-Isua area during this time span, which are directly related to the present study.

B. Geology at Isua

Within the confines of the Isua area itself, three major lithologic units are present: the Isua supracrustals, the Amitsoq gneisses and the Ameralik dykes. Figure 2 shows the general field relations between each of the units. The geology of the area has been extensively described in the literature (cf. references listed in prior section), and the reader is referred to these publications for the detailed description. However, to acquaint those readers unfamiliar with the geology of the Isua area, a brief description and discussion of the rocks are presented herein.

Isua Supracrustals

The Isua supracrustal belt forms an arcuate belt, 10 to 20 kilometres in diameter, surrounding a dome of Amitsoq gneiss. The belt presents itself with variable thickness, reaching a maximum width of nearly two kilometres near the margin of the inland ice sheet, thinning to approximately one kilometre across near Lake Imarssuaq (Allaart, 1976b; Bridgwater *et al.*, 1976). Contacts of the various units within the belt follow the overall general structural trend, displaying intermediate to high angle dips to the southeast.

To the west, the belt is truncated against the gneisses by the Ataneq fault and to the east by the inland ice sheet. Near the ice sheet, a banded ironstone formation yielded a Pb-Pb whole rock isochron age of $3,760 \pm 60$ Ma (Moorbath *et al.*, 1972, 1975). Recent work has yielded a Sm-Nd isochron age of 3,770 Ma (O'Nions, 1979) for the gabbroschiefer unit and similar U-Th-Pb ages on zircons from the acid volcanics

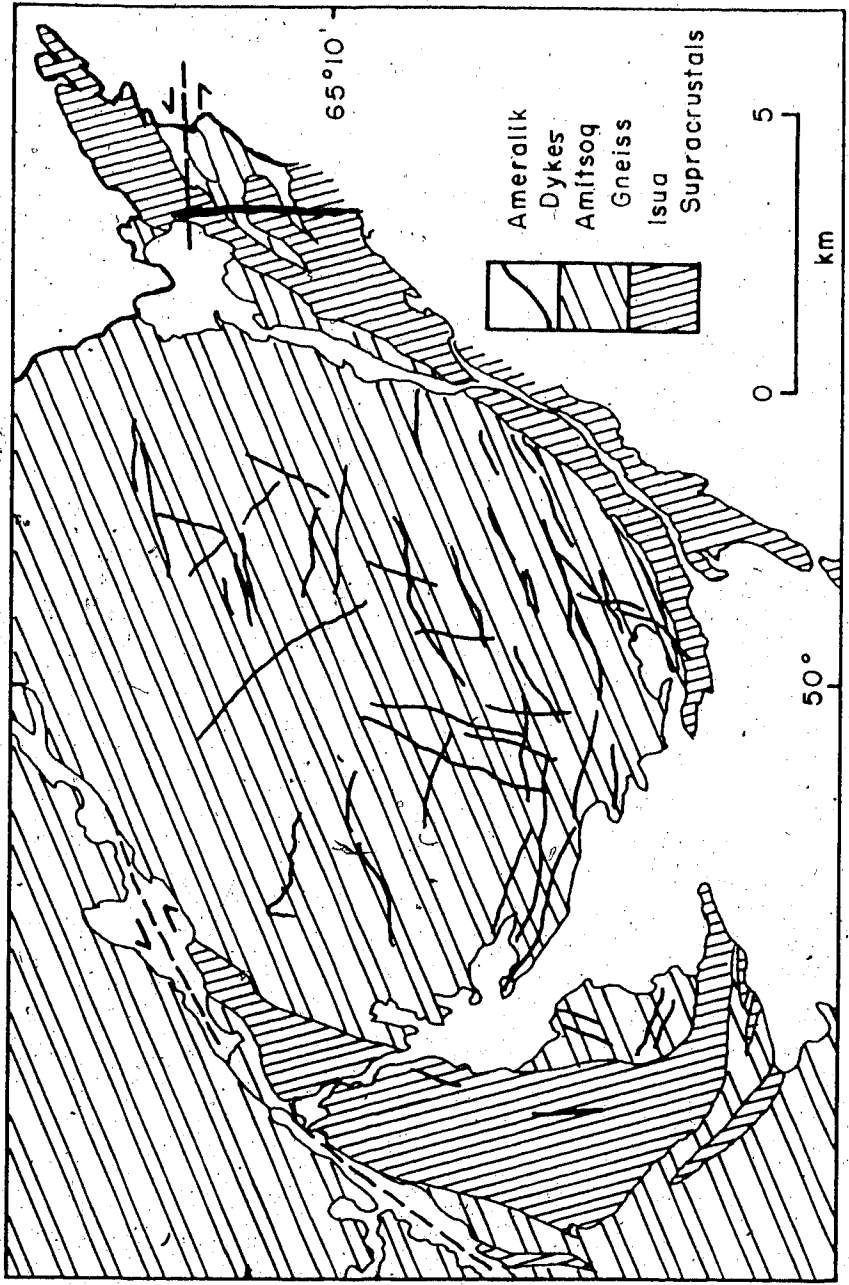


Figure 2: General geology of the Isua area showing the three major lithological units present.

sediments in the upper part of the succession at Isua (Michard-Vitrac, *et al.*, 1977).

Work by Allaart (1976a) and Nutman *et al.* (1982) has done much to elucidate the geology within the supracrustal succession. Seven major lithologies are described: amphibolites, cherts (quartzites with no evidence of detrital origin), ironstones, felsic detrital rocks, banded calcareous rocks, ultramafic rocks (and their metamorphic equivalents) and the garbenschiefer unit, a chloritic leucoamphibolite with high Mg-Al contents.

Two sedimentary sequences within the succession have been recognized (Nutman *et al.*, 1982). Sequence A is composed of the layered amphibolite, chert, banded ironstone, banded calcareous and felsic detrital units. The sequence is interpreted as representing a cycle of basic volcanic activity with associated formation of chemical sediments (komatiitic association?) to felsic detrital sedimentation resulting from the breakdown and weathering of acid volcanic deposits.

Sequence B, composed of a layered felsic detrital component and a two mica (biotite-chlorite) garnet-staurolite schist, represents a transition in deposition from felsic detrital sediments to pelites derived from the decomposition of more basic volcanics.

Amitsoq Gneiss

The Amitsoq gneiss, defined by Black *et al.* (1971) and McGregor (1973), is the older of two major occurrences of quartzo-feldspathic gneiss which crop out in the Godthaabsfjord-Isua area. The major feature which serves to distinguish the Amitsoq from the younger Nuk gneisses is the presence in the Amitsoq gneisses, of abundant amphibolite bodies derived from basic dykes, named Ameralik by McGregor (1968, 1969). The Nuk gneisses are not cut by the Ameralik dykes.

Extensive work on these gneisses based on geology (McGregor, 1968, 1969, 1973, 1979; McGregor and Bridgwater, 1973; Bridgwater and McGregor, 1974; Chadwick and Coe, 1976; Myers, 1976; Bridgwater *et al.*, 1979), geochemistry and geochronology (Moorbath *et al.*, 1972, 1977; Baadsgaard, 1973, 1976; Moorbath, 1975; Baadsgaard *et al.*, 1976; Lambert and Holland, 1976; Moorbath and Pankhurst, 1976; Kalsbeek, 1981) have revealed much of the early history of the area and its later development.

Metamorphism outside the supracrustal belt at Isua has reworked the gneisses to such an extent that primary structures and characteristics are often no longer recognizable. The gneisses appear as large units of inhomogeneous rocks with well developed, thin pegmatite layering (Bridgwater *et al.*, 1976), and contain numerous metabasaltic bodies, mostly reworked Ameralik dykes (McGregor, 1973; Gill and Bridgwater, 1975). The rocks are predominantly quartz-oligoclase-biotite gneisses, believed derived from parents with tonalitic-trondhjemitic affinities (McGregor, 1973, 1979).

The Amitsoq gneiss at Isua, shown to be polygenetic in nature (Bridgwater *et al.*, 1976) often preserve primary igneous textures. They are composed of two distinct phases, differing in mafic content, feldspar type and relative colour index. The lighter phase intrudes the darker. Subsequent mapping by Nutman *et al.* (1982) within the gneissic dome, has further subdivided the two major units of the gneiss as follows:

- I) Grey gneisses (oldest). Grey, weakly banded, polyphase, plagioclase flecked tonalitic to granodioritic gneiss with sparse pegmatite banding. Makes up approximately 60 percent of the complex.
- II) Thin grey gneiss sheets. Rare, thin, fine grained tonalitic sheets cutting (I).
- III) Early dykes (named Tarsartoq by Nutman, 1982). Biotite-amphibolite and mafic dioritic dykes, less than 2 metres wide, cutting both (I) and (II).
- IV) White gneisses. Granitic and pegmatitic homogeneous to schleiritic pale gneisses, forms the bulk of the remainder of the complex. Intrudes (I)-(III).
- V) Late thin grey sheets. Homogeneous grey tonalitic sheets intruding (I)-(IV).

Toward the outer margin of the gneissic dome, the relatively undeformed nature of the gneisses, and the individual nature of the lithologies present change and gradually become less distinct. Just beyond the arc of the supracrustal belt, the gneisses assume the appearance of similar rocks found outside Godthaab (McGregor, 1973; Nutman *et al.*, 1982) and have been directly correlated with these rocks on this basis.

Deformation and attenuation of the gneisses to conform to the arcuate structure of the supracrustals near the contact is postulated by Moorbath *et al.* (1975) to have

occurred soon after emplacement of the original parent magma since there was (at that time) no geological or geochronological evidence supporting tectonic or thermal alteration of the rocks later than 3,600 Ma (Baadsgaard, 1973, 1976).

Ameralik Dykes

The primary concern of this study, the Ameralik dykes are some of the youngest rocks which crop out in the Isua area (McGregor, 1968, 1969; Gill and Bridgwater, 1976). Their age (cf. geochronology references cited previous section), although not established, is believed to lie between 3,600 Ma and 3,100 Ma, based on dating of the Amitsoq and Nuk gneisses.

Within the gneissic dome at Isua, relatively (physically) well preserved dykes are abundant. They intrude the country rock in two distinct swarms. One trends nearly East-West and the other North-South. They are known to intersect each other, but no age relationship between them has been established (McGregor and Bridgwater, 1974). The east-west dykes are short podiform structures while dykes from the other swarm are elongate and narrow (cf. figure 19, Bridgwater *et al.*, 1976, p. 33). The physical appearance of the dykes has been attributed to emplacement of the dykes into plastic country rocks during deformation, (Bridgwater *et al.*, 1976).

Follow-up work by Nutman *et al.* (1982) has shown there to be three principal swarms:

- I) NNE-SSW dykes with ultramafic affinities. Some relict olivine and pyroxene present in the undeformed dykes, altering to talc-schists with progressive deformation.
- II) Intersecting dyke sets. Vertical to southerly dipping, possibly conjugate. Gradual increase in the amount of deformation with approach to, and intrusion of, the supracrustal belt.
- III) N-S trending metadolerite dykes, locally with plagioclase megacrysts. Highly discordant angle of intersection with host deformed gneisses near supracrustals and seemingly little deformed. Proximal (2-3 kilometres) to the supracrustals, slight mineralogical lineation within the dykes has been noted.

Further from the contact of the gneisses with the supracrustals, the dykes appear to retain their primary igneous texture. General petrography of the dykes has been previously described (Gill and Bridgwater, 1975; Bridgwater *et al.*, 1976). The petrography of specific dykes sampled for this study will be described and discussed in the next chapter.

III. SAMPLING AND PETROGRAPHIC DESCRIPTIONS OF ISUA DYKES

A. Introduction

The study by Gill and Bridgwater (1979) showed the dykes at Isua form a very cohesive geochemical and petrochemical group. They were judged to be similar to primitive, oceanic tholeiites and/or basic island arc volcanics characterized by meteoritic Rare-Earth Element patterns and low K₂O contents.

In the field, macroscopic, local alteration of the dykes is visible along the margins, but does not penetrate to the dyke centres, suggesting that post crystallization alteration has had limited chemical effect on the dykes. It was hoped, based on chemical similarity of the dykes at Isua (Gill and Bridgwater, 1979), that isotopic homogeneity would also be maintained. Petrographic examination has revealed marked disparity in the tectonic style of deformation, degree of recrystallization, mineral assemblages and degree of alteration present both within and between the dykes.

The initial collection of samples for dating, made during the summer of 1978, was random. Single hand specimen sized samples were taken from the centres of various dykes (Fig. 3, random samples). Preliminary petrographic and isotopic work on these samples showed mineralogic and isotopic heterogeneity, and further collection was required.

During August 1981, specimens were collected from separate dykes from three widespread locations within the study area with a view toward examination of isotopic and petrologic homogeneity of single dykes. Samples were taken across margin to margin transects and also longitudinally. A single dyke intruding both gneiss and supracrustal rocks was sampled as a control in examining possible differential contamination contributed to the dykes by the different host lithologies.

B. Mineralogy and Petrology

The initial mineralogy of the dykes is changed; original compositions may be directly inferred from textures, pseudomorphic replacement of pre-existing minerals and alteration product associations. In many cases, primary textures and crystal habit have been preserved and the ensuing changes have amounted to little more than degradation

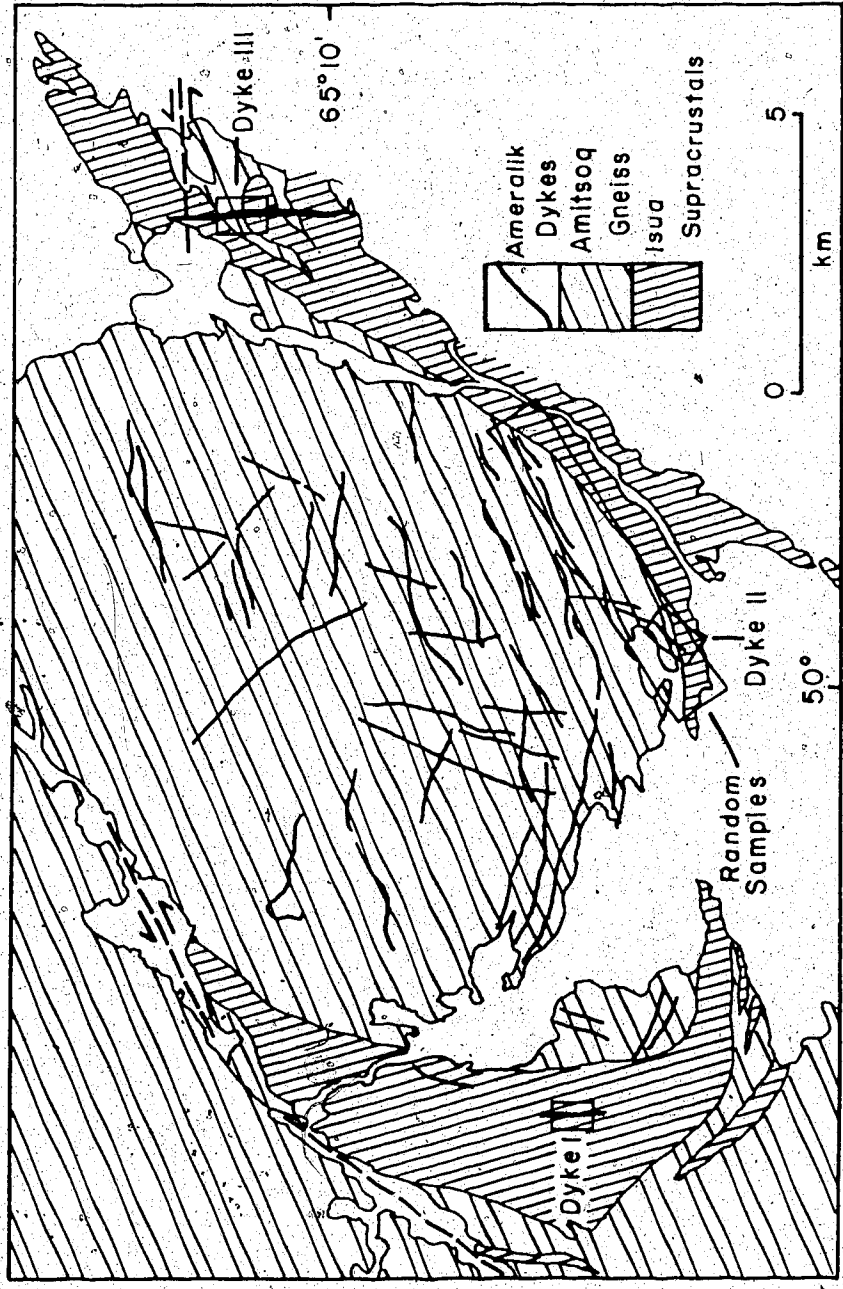


Figure 3: Collection locations for the random samples and Dykes I, II and III.

of the higher-temperature ferro-magnesian minerals. In other instances, complete recrystallization of the component minerals has occurred, but original compositions may be estimated from less severely altered samples from within the same area.

Dyke I

Samples taken from a dyke within the Isua supracrustal belt (225952A-F, 292234A-P) lying along the west side of the gneissic dome, (see Figure 3), display a distinctive mineral assemblage. West to east sections through the dyke show progressive increase in the degree of scapolitization toward the dyke centre, while preserving the original plagioclase feldspars nearer the contact of the host gabbro unit. The scapolite displays chemical and mineralogical changes as well. Scapolite at the dyke margin, found in association with andesine feldspar, is predominantly marialite ($3\text{NaAl}_2\text{Si}_2\text{O}_7 \cdot \text{NaCl}$) but grades inward toward the meionite ($3\text{CaAl}_2\text{Si}_2\text{O}_7 \cdot \text{CaCO}_3$) end member (possibly reaching as calcic a composition as mizzonite (Me_{60})).

Scapolitization is believed to involve the complete recrystallization of the dyke. This is shown by strongly pleochroic green amphibole (displaying true amphibole crystal habit) coexisting with the scapolite. Contacts are sharp and no grain corrosion is visible. Pale green hornblende, pseudomorphic after clinopyroxene was noted in the core of the dyke. Massive in appearance in plane polarized light, the amphiboles (as well as the scapolite) appear to be quite granular under crossed nicols (Plates 1-4). Vigorous recrystallization of the original minerals has occurred and in some cases, clinozoisite cores are surrounded by large aggregates of scapolite, possibly indicating decomposition of an original more calcium-rich plagioclase. In several instances, plagioclase feldspar has recrystallized (Plates 1 and 2), though to a much lower anorthite content than originally present (Krupicka, pers. comm.).

Skeletal ilmenite-magnetite fragments are found associated with the amphibole, suggesting formation during the recrystallization at the expense of the parent pyroxenes (Deer *et al.*, 1966). Incipient biotite is sporadically found rimming the ilmenite-magnetite grains and indicates retrogressive processes were weakly active after the major recrystallization period.

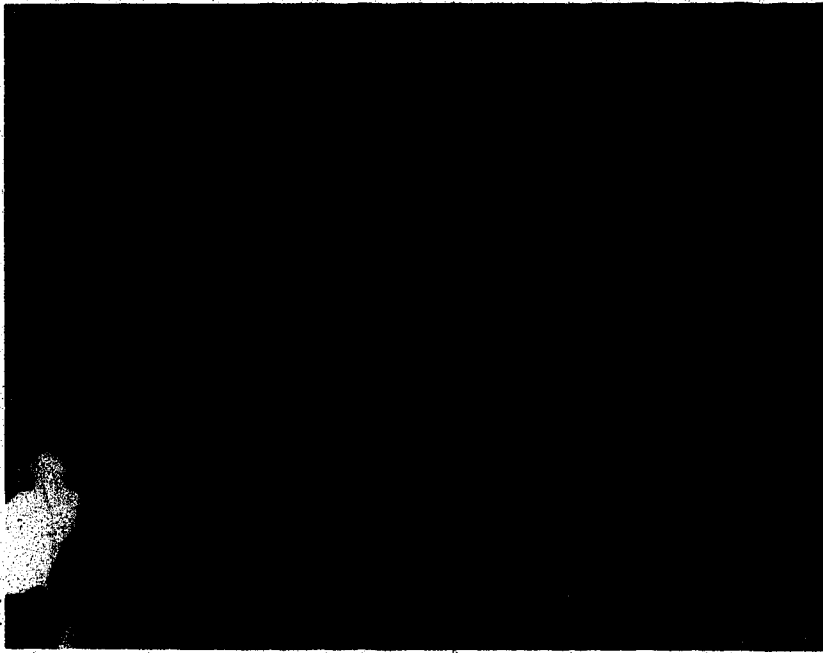
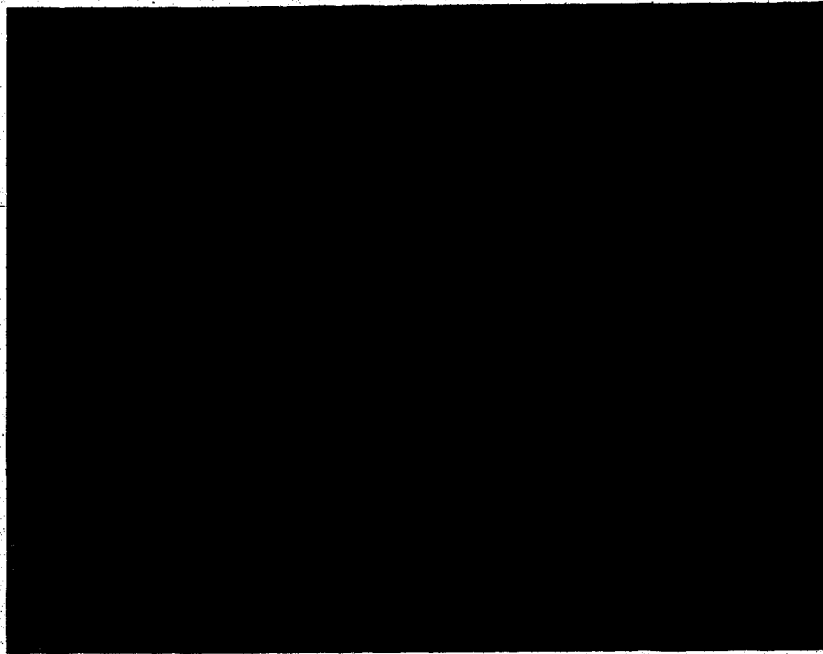


Plate 1: Dyke I (top); Recrystallized hornblende and feldspar with scapolite and clinozoisite, x40, plane polarized light.

Plate 2: Dyke I; Recrystallized hornblende and feldspar with scapolite and clinozoisite, x40, crossed nicols.



Plate 3: Dyke I (top): Recrystallized hornblende with clinozoisite/epidote clots, no evidence of feldspar, x40, plane polarized light.
Plate 4: Dyke I; Recrystallized hornblende with clinozoisite/epidote clots, no evidence of feldspar; x40, crossed nicols.

Limited appearance of allanite was noted in several specimens from the western margin of the 292234 series, accompanying the epidote group replacement of the feldspars. Allanite formation is possibly associated with late stage, hydrothermal activity along the dyke margin as the recrystallization event waned.

Dyke II

The samples which were of the most interest were taken from a dyke (292229 series) situated along the southern margin of the gneissic dome, extending into the supracrustal belt and intersecting several different lithologies within the supracrustals (Figure 4). Two margin-to-margin traverses of the dyke were made, one where the dyke intruded the gneiss and one where it intruded the supracrustals. A longitudinal sampling traverse was made along the dyke between the two margin-to-margin traverses. The primary purpose in such a collection was to examine the possibilities of differential isotopic and chemical contamination imparted to the dyke via assimilation of pre-existing crustal material during emplacement or subsequent regional metamorphism.

Textural and mineralogic examination indicate this particular dyke has not suffered any appreciable metamorphism since emplacement. Thin sections show retention of primary ophitic textures with laths of plagioclase and aggregates of pale green hornblende replacing clinopyroxene (Gill and Bridgwater, 1979). In some dyke core samples, hornblende replacement of the clinopyroxenes is incomplete (Plate 5) and some samples show little effect of any retrograde alteration. Iron rich olivine is associated with these less altered samples. The presence of fresh clinopyroxene and olivine suggests that low-grade hydrothermal alteration processes were not pervasive enough to effect total alteration throughout the dyke.

Samples numbered 292229A-L, correspond to the west to east traverse across the dyke where hosted by the Amitsoq gneiss (Figure 3). As with samples from the previous dyke, there is no microscopic evidence indicating onset of dynamic metamorphic processes. Although jointing is visible in a small percentage of the hand specimens, it has no apparent affect on the microfabric of the rocks.

In Dyke II, static retrogression of the clinopyroxene to poorly developed amphibole aggregates appears to be the major alteration process. Formation of skeletal

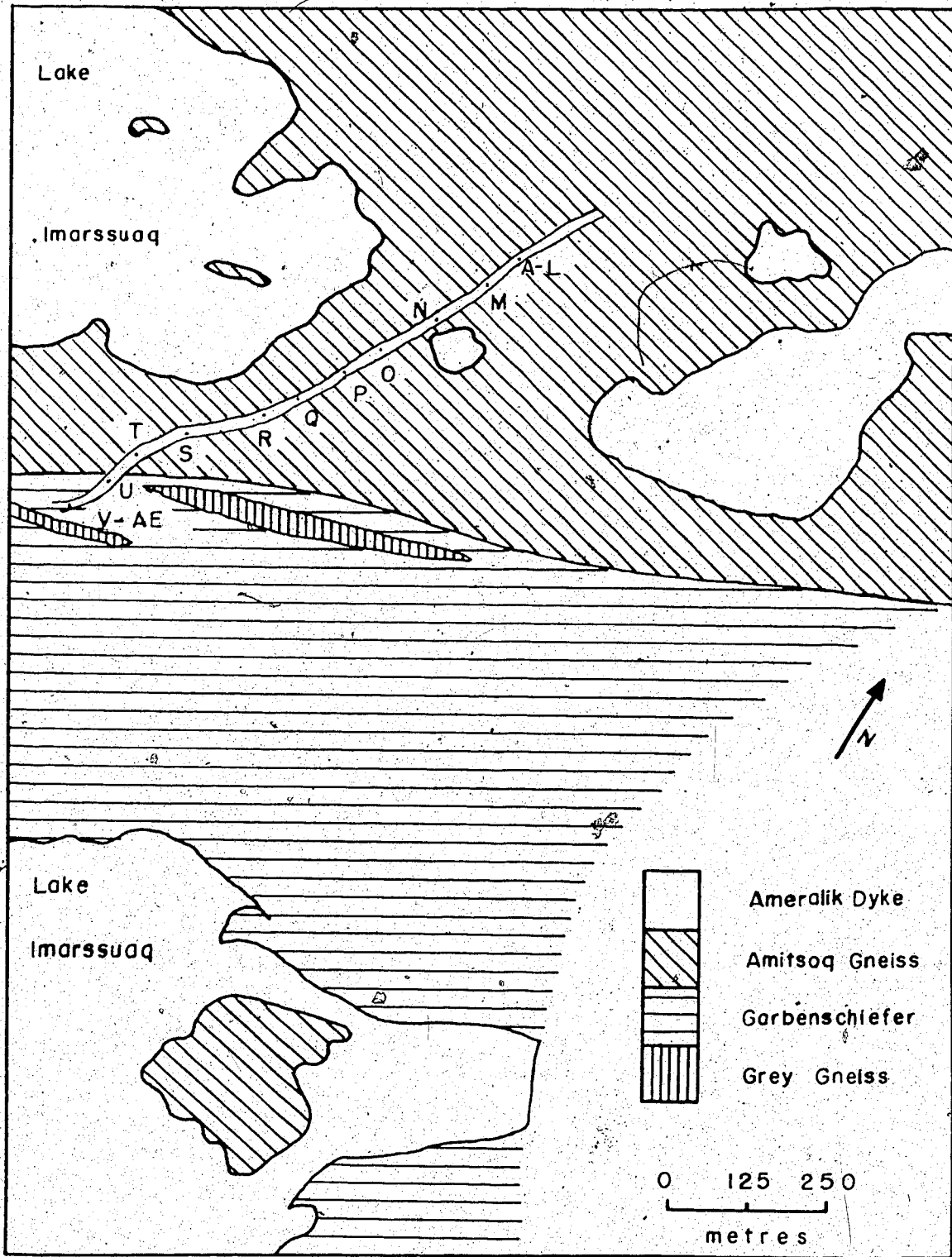


Figure 4: Sample locations; Dyke II.

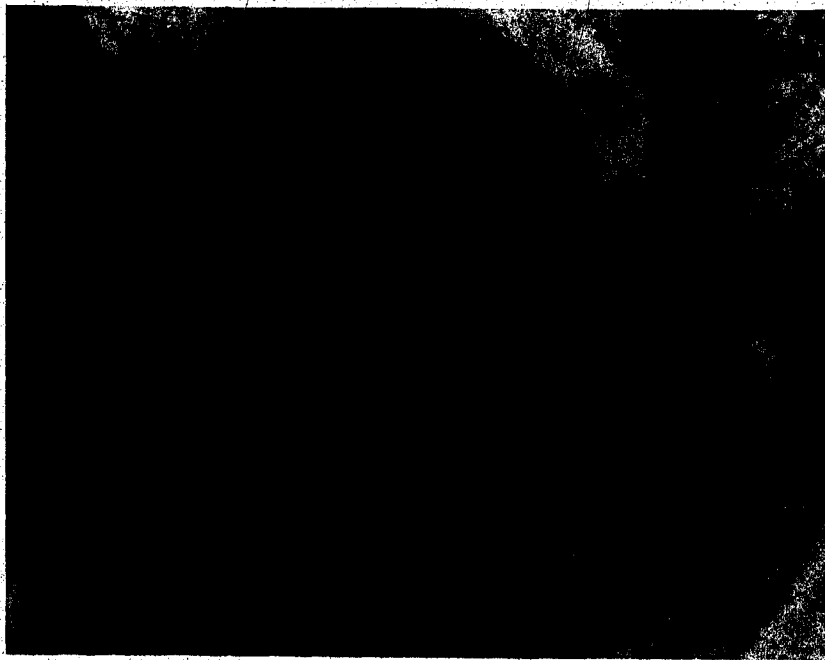


Plate 5: Dyke II (top); Clinopyroxene altering to hornblende, slight uralitic alteration of the clinopyroxenes is also visible, x40, plane polarized light.

Plate 6: Dyke II; Olivine altering to serpentine group minerals (antigorite-lizardite?), enclosed in clinopyroxene, x40, plane polarized light.

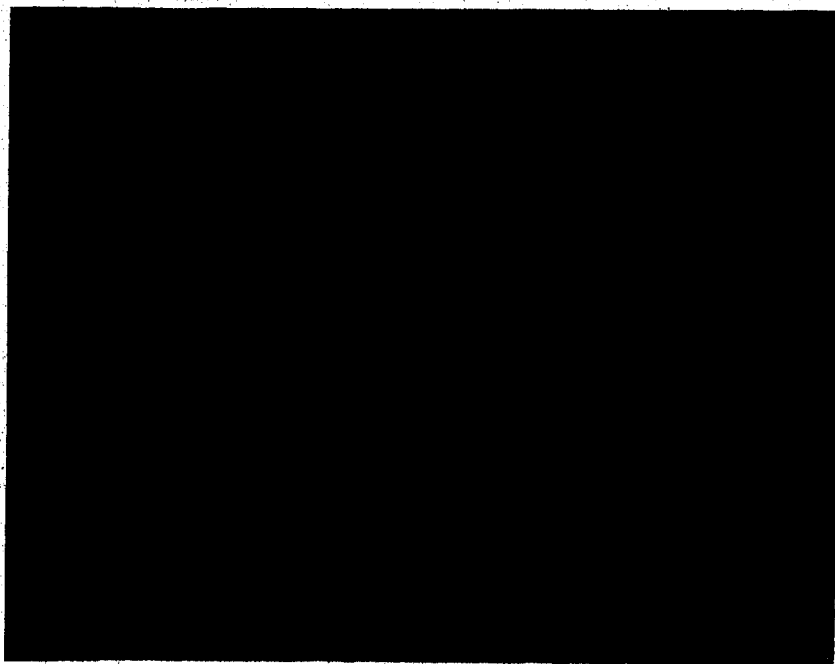


Plate 7: Dyke II (top); Ilmenite-magnetite altering to sphenes in turn to biotite, x40, plane polarized light.

Plate 8: Dyke II; Development of uralitic and alkali alteration in clinopyroxene and amphibole, x40, plane polarized light.

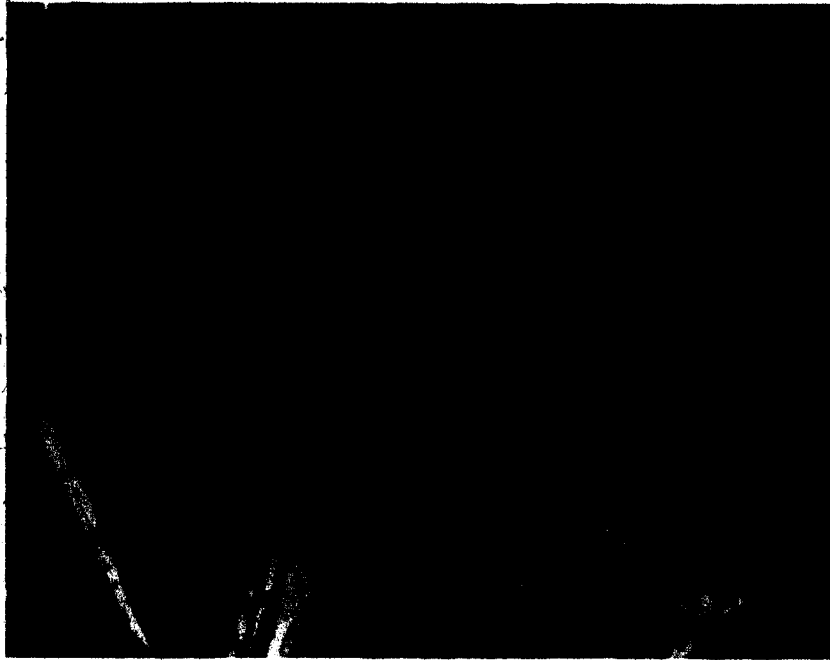


Plate 9: Dyke II (top); Development of uralitic and alkali alteration in clinopyroxene and amphibole, x 40, crossed nicols.

Plate 10: Dyke III; Primary micropegmatite, zoned plagioclase and clinopyroxene, x40, crossed nicols.

ilmenite-magnetite grains again accompanies clinopyroxene degradation. The amphibole content of Dyke II is much greater than Dyke I, attaining almost 75 percent in certain samples.

Other lines of evidence indicating low-grade, post-magmatic hydrothermal alteration include limited presence of serpentine group minerals (antigorite-lizardite?) associated with the breakdown of olivine (Plate 6), rims of sodic amphibole (arfvedsonite?) encrusting patches of green amphibole aggregate, Fe-Ti oxides altering to sphene and in turn into biotite (Plate 7), and most importantly, the presence of uralitic pyroxene (Plates 8 and 9). The presence of uralite may be ascribed to the action of hydrothermal solutions which may be associated with the late stage crystallization sequence of igneous rocks, or to post consolidation processes unrelated to the igneous activity from which the rocks were derived. In the latter case, the uralitization may be associated with regional, thermal or metasomatic metamorphism (Deer *et al.*, 1966). Also supportive of the case for limited metasomatic metamorphism is the sporadic appearance of scapolite (mainly dipyre (Me_{30})). Epidote group mineralization is not as pervasive as described for Dyke I, and the presence of free carbonate is noted throughout samples from this particular transect. Radiating clusters of chlorite (clinochlore?) partially replace amphibole aggregates and are not associated with any microfractures or veining.

Erratic appearance of scapolite, arfvedsonite(?), chlorite and biotite indicate the dyke also suffered incomplete low-grade hydrothermal alteration, which appears to have been more intense in certain places. Here also are the first indications of true tectonic deformation of the rocks. Along most of its length, the long axis of the dyke strikes approximately obliquely to the regional geologic structure, but as it approaches the southern margin of the gneissic dome, near the contact with the supracrustal belt, the dyke curves to align partly with the arcuate form of the supracrustals. Once penetrating the supracrustals, the oblique trend of the dyke returns. Sample 292229S details marked shearing and foliation, accompanied by more intense recrystallization and alteration, more clearly representative of samples found within the 292234 suite.

Samples taken from the dyke where hosted by the supracrustal sequence (292229U-Z, AA-AE) display mineralogic, textural and alteration patterns similar with

samples from the opposite end of the dyke hosted by the gneisses. The major distinction is the absence of scapolite, coupled with an increase in the percentage of epidote group minerals present.

Dyke III

At the eastern margin of the study area, a major "Proterozoic" dyke was sampled in a manner similar to the previous dykes (Samples 292289A-R). Figure 5 shows the location of the samples taken laterally and along the dyke centre. Two specific features of this dyke serve to distinguish it from the others; it is the thickest and most extensive dyke, sampled entirely within the supracrustals, and it is the only dyke sampled which extends far enough to the south to exit the supracrustal belt and intrude the highly deformed gneissic complex beyond.

Distinctive features of these samples include true doleritic texture comprised of very coarse clinopyroxene crystals, often completely surrounded by porphyritic andesine feldspars. The feldspars, however, are heavily saussuritized. This is the only sign of any epidote group mineralization throughout the dyke. The clinopyroxenes, which comprise up to 40 percent of each sample, are found in various stages of mild to extreme uralitization, and show little evidence for the degradation to green amphibole common among the Ameralik dykes. The most striking feature of these samples is the presence of up to 15 percent interstitial, primary micropegmatite, often surrounding the feldspar phenocrysts. The feldspar intergrowths within the micropegmatite show signs of sericitization (Plate 10). The same plate also shows contacts at the grain boundary between the feldspar and the micropegmatite are sharp and planar, indicating that no feldspar exsolution has occurred and that the two components grew in thermal equilibrium.

Presence of arfvedsonite(?) rims surrounding the clinopyroxene, intense uralitization of the clinopyroxenes, minor sericitization of the micropegmatite feldspar and saussuritization of the feldspar phenocrysts again indicates that post-magmatic, metasomatic and/or hydrothermal alteration processes were active during or soon after emplacement. There is very little evidence of retrograde metamorphism.

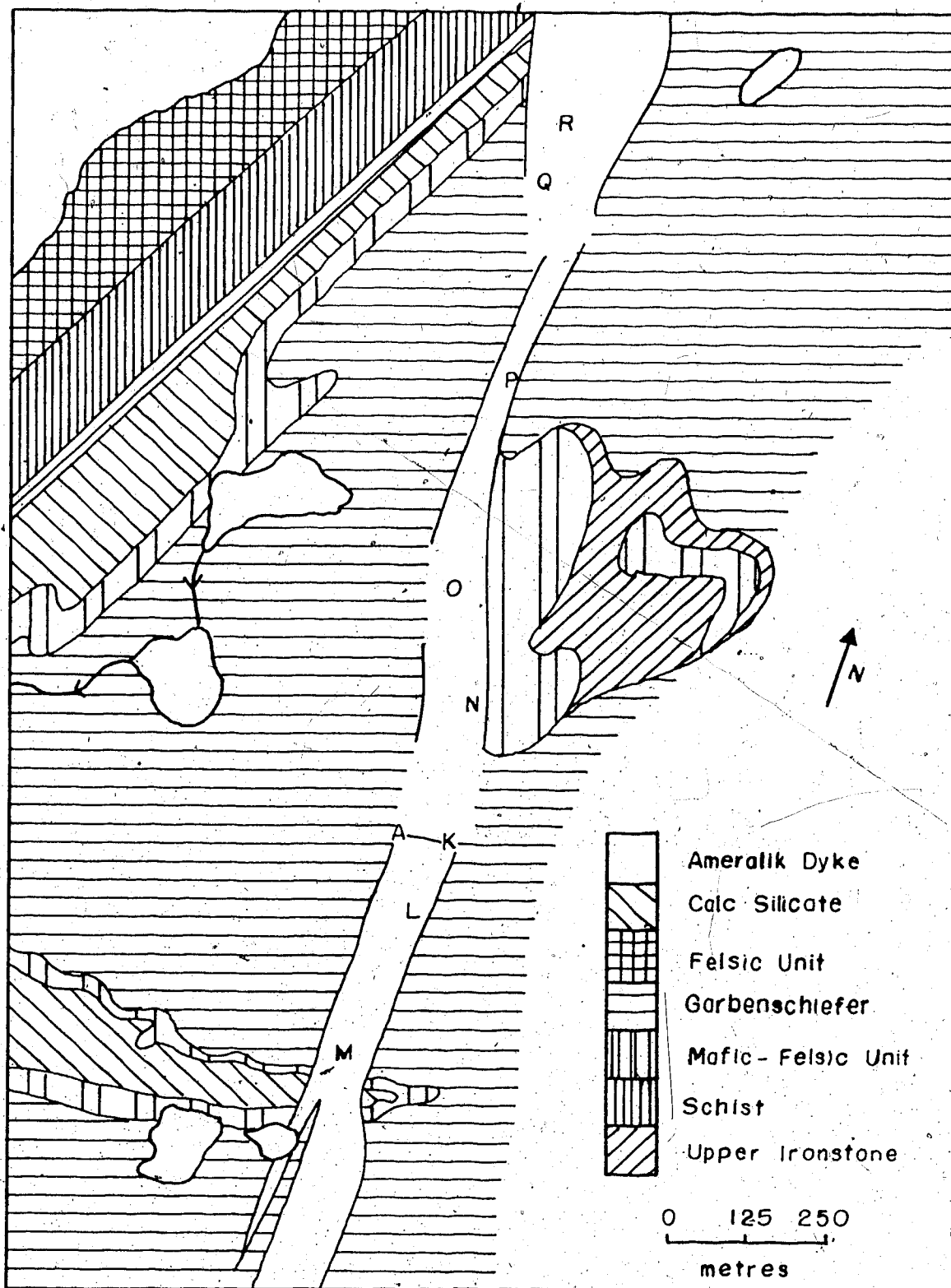


Figure 5: Sample locations; Dyke III.

Unlike the previous dyke samples, the texture and mineralogy of these dyke samples are fairly uniform throughout. The presence of clinopyroxene, aldsine phenocrysts and primary micropegmatite indicate the dyke enjoyed an extended cooling period compared to the other dykes studied. It is apparent that felsic minerals had a longer cooling history than did the ferro-magnesian minerals. With the exception of one sample (292289L) collected from the eastern dyke margin, all samples are essentially mineralogically homogeneous.

Random Samples

Interpretation of data from separate locations is a difficult task, especially when wide discordance exists among the isotopic data. The original collection consisted of samples from 24 individual dykes which intrude both major lithologies, some of which are found to extend beyond the undeformed enclave (McGregor, 1973). Samples used for the earlier analyses were chosen on their positions relative to the undisturbed 3,700 Ma. enclave. Samples taken from outside this region were rejected and those which remained can be described relative to the different dykes previously described. Microscopic characteristics of the samples appear to be randomly distributed. All features described from earlier dykes have been found in these independent samples, the locations of which (Figure 3) are close enough that spatial differentiation or classification based on location and physical appearance is impossible. There is simply too much overlap of textures, alteration and mineral components to establish any specific divisions.

C. Summary

It has been shown that the Ameralik dykes at Isua possess variable mineralogy and textures. Although it has been proven that dykes collected from the general location within the unmetamorphosed enclave defined by the belt of Isua supracrustals are chemically similar based on trace and REE distribution patterns (Gill and Bridgwater, 1979), there is little similarity in mineralogic composition. Metamorphic processes which have been active in the Isua area have differentially affected each individual dyke. Consistency in alteration is lacking and clear cut relations between dyke rock, host lithology and sample location can not be established.

Scapolitization predominates over uralitization in some locations, yet the processes leading to the different alteration products are not mutually exclusive. Some dykes display pervasive and thorough alteration and no evidence of recrystallization, others present exactly the opposite. One factor in common with all samples is the positive evidence for limited migration of alkalis associated with one of two processes; either hydrothermal activity in conjunction with late stage crystallization of igneous rocks, or metasomatic metamorphism on a regional scale indicated by the presence of alkali amphibole in each sample.

Clearly, conclusions regarding the history, identity and classification or grouping of the Ameralik dykes can not be based solely on petrographic means. It is therefore necessary to utilize additional parameters before arriving at any conclusions.

IV. ANALYTICAL

During the course of this study, 101 samples were analyzed for their Rb and Sr isotopic compositions and 100 for their Pb isotopic composition.

Samples were prepared by HF-HNO₃ decomposition, Ba(NO₃)₂ coprecipitation of Sr and Pb (H⁺ cation and Cl⁻ anion exchange purification of each respectively), and H₂SO₄ treatment, ignition and extraction for Rb. Complete sample chemical and analytical procedures are discussed by Chaplin (1981) and are briefly described in Appendix II.

Rb/Sr

A single analysis on the NBS 607 standard reference feldspar yielded the following results:

$$^{87}\text{Sr}/^{86}\text{Sr} = 1.20088 \pm 0.00005; \text{Sr ppm} = 67.0; \text{Rb ppm} = 521.2$$

in good agreement with the certified values of;

$$^{87}\text{Sr}/^{86}\text{Sr} = 1.20039 \pm 0.00002; \text{Sr ppm} = 65.5 \pm 0.3; \text{Rb ppm} = 524.0 \pm 1.0$$

Repeated analyses on the SRM 987 Bureau of Standards strontium standard gave the following results;

$$^{87}\text{Sr}/^{86}\text{Sr} = 0.71035 \pm 0.00006; 0.71022 \pm 0.00004; 0.71018 \pm 0.00003$$

These agree variably with the accepted value of 0.71014 ± 0.00002 . In most cases a normalization correction factor would be applied to the data to bring it them in line with an SRM 987 normalized value of 0.71014, but due to sporadic technical and equipment problems with the analytical facilities, no normalizing factor was calculated or applied to the raw data. Had it been done, the resultant lowering of the measured $^{87}\text{Sr}/^{86}\text{Sr}$ ratios by 0.017% would not significantly alter the position of any of the data points.

Replicate analyses of samples for Rb and Sr (see Table 1) indicate analytical precision for Sr isotopic analyses of approximately $\pm 0.04\%$ of the measured $^{87}\text{Sr}/^{86}\text{Sr}$. Rubidium isotopic ratios cannot be exactly corrected for fractionation and are, therefore accurate to within only $\pm 0.3\%$. Replicate analyses indicate precision for Rb analyses is 0.257%, neglecting fractionation effects.

Rb and Sr blanks determined by the author and other workers from this laboratory, have established average blank levels of approximately 2.7 ng Rb and 1.1 ng Sr. These blank levels (combined with analytical accuracy determined) have no significant effect on the raw data, therefore no blank correction has been applied.

Pb/Pb

Duplicate analyses on six Pb samples (see Table 2) are in fair to excellent agreement with each other. The data indicate analytical precision of 0.02% to 0.32%. The difference in results is mainly attributed to technical difficulties encountered with the analytical facilities during this study.

Lead results have been corrected for fractionation effects by utilizing the following normalization constants determined by repetitive analyses on a National Bureau of Standards SRM 981 lead standard by D. Krstic (1981):

$$^{206}\text{Pb}/^{204}\text{Pb} \times 1.002918$$

$$^{207}\text{Pb}/^{204}\text{Pb} \times 1.004414$$

$$^{208}\text{Pb}/^{204}\text{Pb} \times 1.006224$$

Analytical precision on individual lead analyses, also determined by Krstic (1981) are given here:

$$^{206}\text{Pb}/^{204}\text{Pb} \pm 0.05\%, \quad ^{207}\text{Pb}/^{204}\text{Pb} \pm 0.07\%, \quad ^{208}\text{Pb}/^{204}\text{Pb} \pm 0.10\% \text{ at the 1 sigma level.}$$

Total lead blank, determined in the laboratory by the author and other workers ranged from 3.0 ng Pb to 4.0 ng Pb. Total whole-rock lead concentrations, although not determined during this study, are estimated to range from 3-10 ppm. Lead blanks of less than one part per mil have no significant effect on the measured isotopic ratios. If they are applied, the variation introduced in the measured ratios would still lie within analytical error, given the range in measurements displayed by the replicate analyses. Therefore no overall blank correction has been applied to the data.

V. RESULTS AND DISCUSSION

For the purpose of this study, it was felt that both Rubidium-Strontium and Lead-Lead whole rock isotope studies should be undertaken with the hope that together, the isotopic systematics of the two methods would shed some light on the age of emplacement of the Ameralik dykes. U-Th-Pb was not attempted due to the naturally low U-Th/Pb ratios characteristic of tholeiitic basalts. The aphanitic nature of the basalts increase the difficulty in obtaining clean mineral separates for mineralogical isotope studies. Sm-Nd methodology, in initial development stages in this laboratory, was not available for use.

Originally, it was hoped that through use of the Rb-Sr method, the age of these Archaean dykes could be obtained in a fashion similar to that for pre-Kenoran dykes which intrude the Canadian Shield (Gates, 1971). Unfortunately, the data presented here exhibit widespread scatter similar to that reported by Davis (1978) at Saglek Bay.

A. Ameralik Dykes, Rubidium-Strontium Results

The Rb-Sr analytical results obtained on the whole rock samples are listed in Table 2 (Appendix I) and the data are plotted on Figures 6-8. For ease of presentation, the data are considered in two groups, one representing samples taken from Dyke I and the other group of samples from Dyke II.

Preliminary inspection of Figure 6 shows the true scatter of the data. Five samples have been omitted from the figure based on petrographic criteria including foliated texture, excess biotite growth and extreme epidote group veining. Samples taken from the random dykes showed marked diversity in their isotopic composition, while samples taken from traverses along and across various dykes display clustering of points (Figures 6-8) with occasional widely variant results. Subdivision of the data points based on several criteria may aid in rationalizing the isotopic behaviour of the rocks.

Figure 9 represents elemental Sr concentration variations within Dyke I as the dyke was sampled from western to the eastern margin. Figure 10 is similar except the data presented is for samples taken across Dyke II. It is interesting to note that dyke

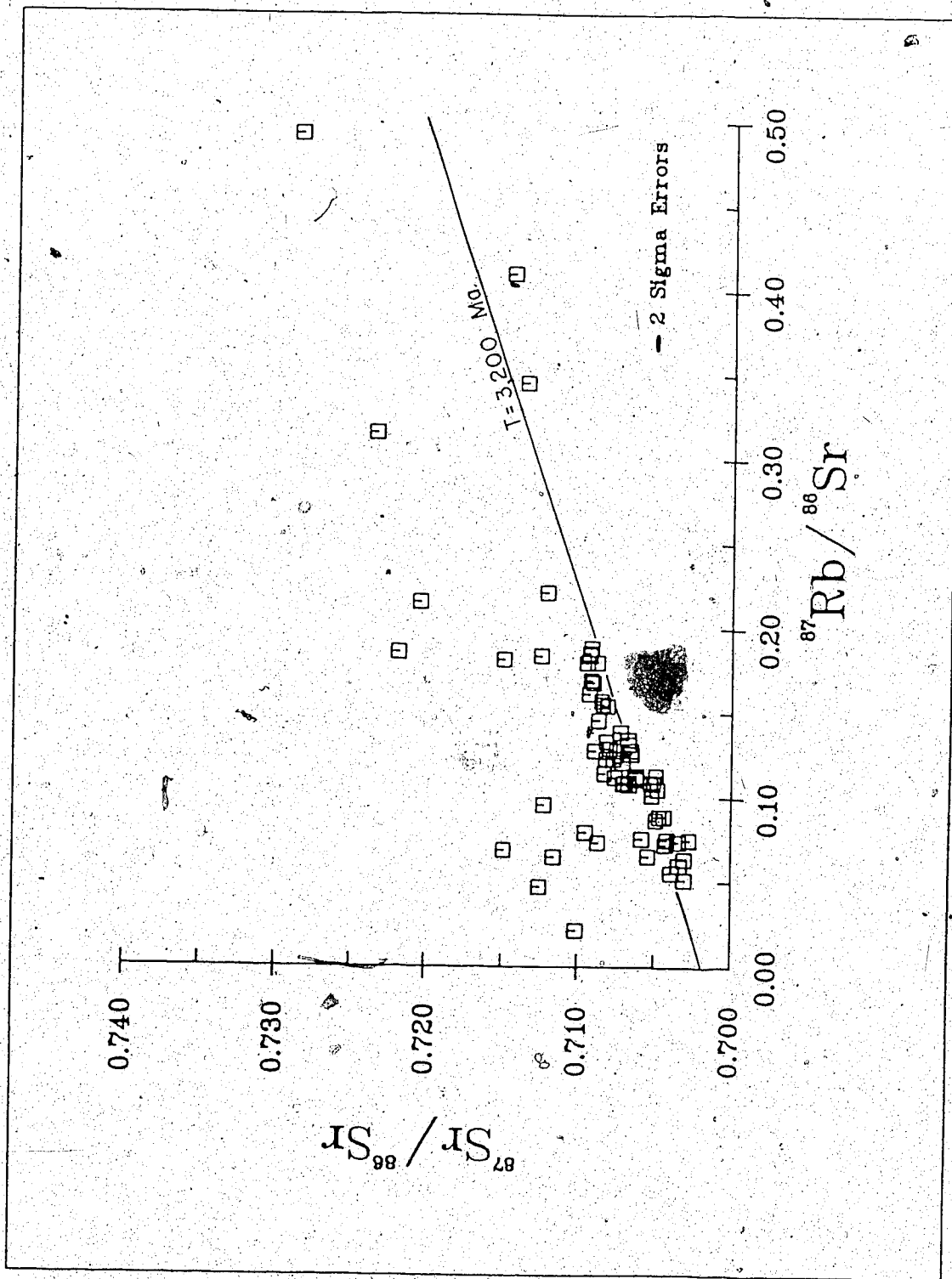


Figure 6: Plot of $^{87}\text{Sr}/^{86}\text{Sr}$ versus $^{87}\text{Rb}/^{86}\text{Sr}$ ratios for the whole rock, Ameralik Dyke analyses.

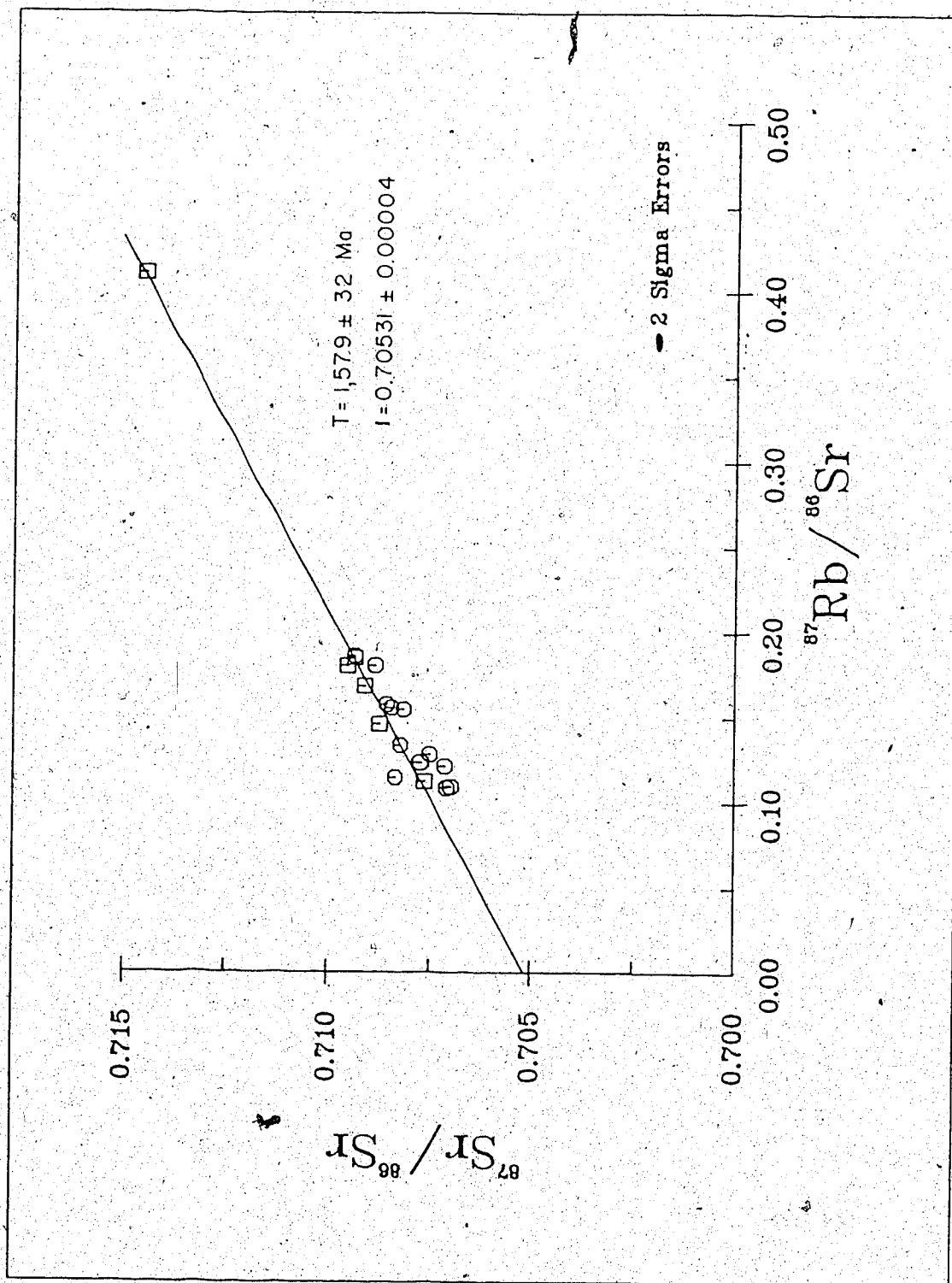


Figure 7: Plot of $^{87}\text{Sr}/^{86}\text{Sr}$ versus $^{87}\text{Rb}/^{86}\text{Sr}$ ratios for Dyke I, original samples represented by squares, follow-up samples by circles.

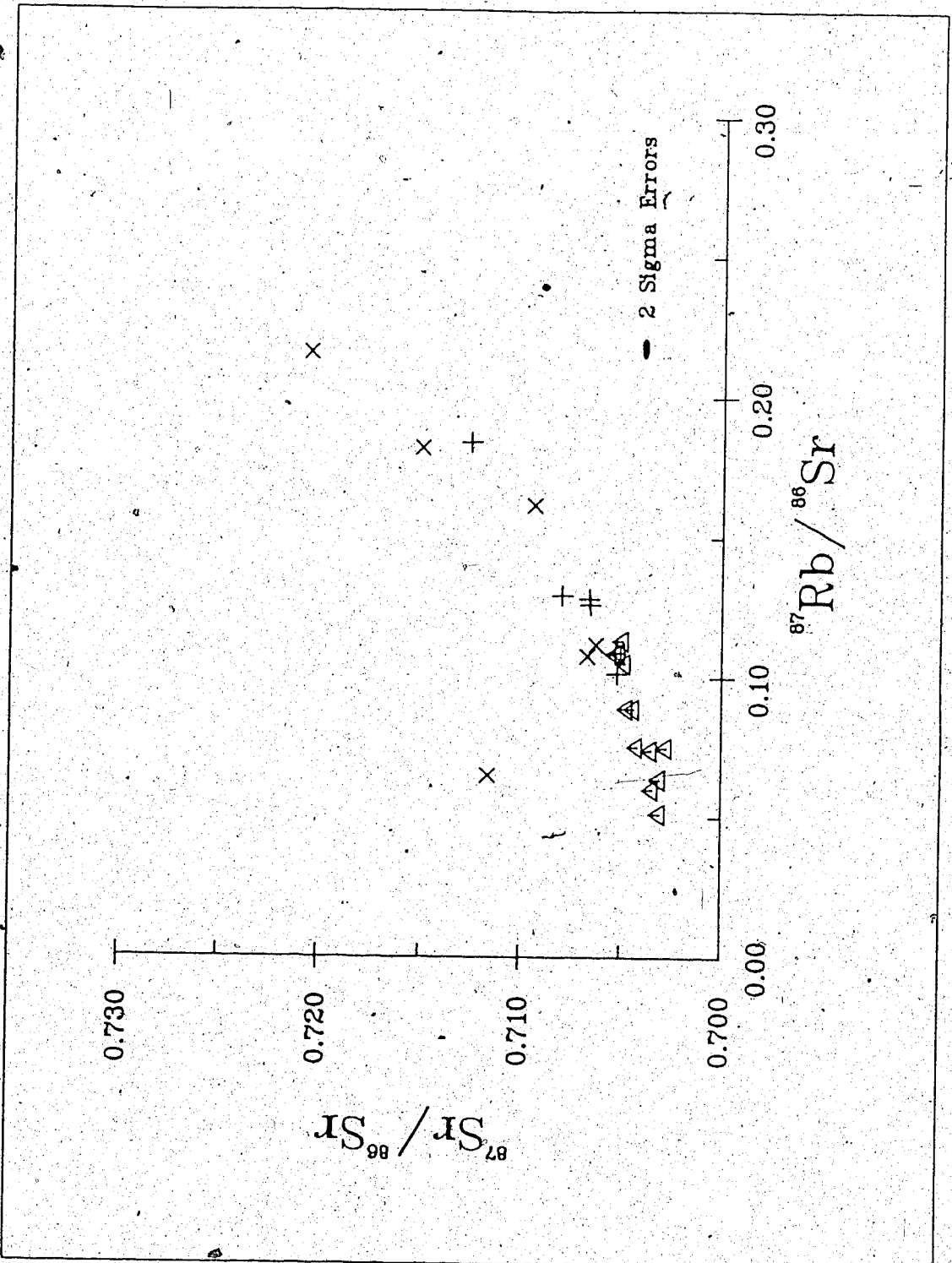


Figure 8: Plot of $^{87}\text{Sr}/^{86}\text{Sr}$ versus $^{87}\text{Rb}/^{86}\text{Sr}$ ratios for Dyke II, triangles represent gneiss hosted W-E traverse; crosses, garbenschiefer hosted traverse; pluses, axial traverse through both lithologies.

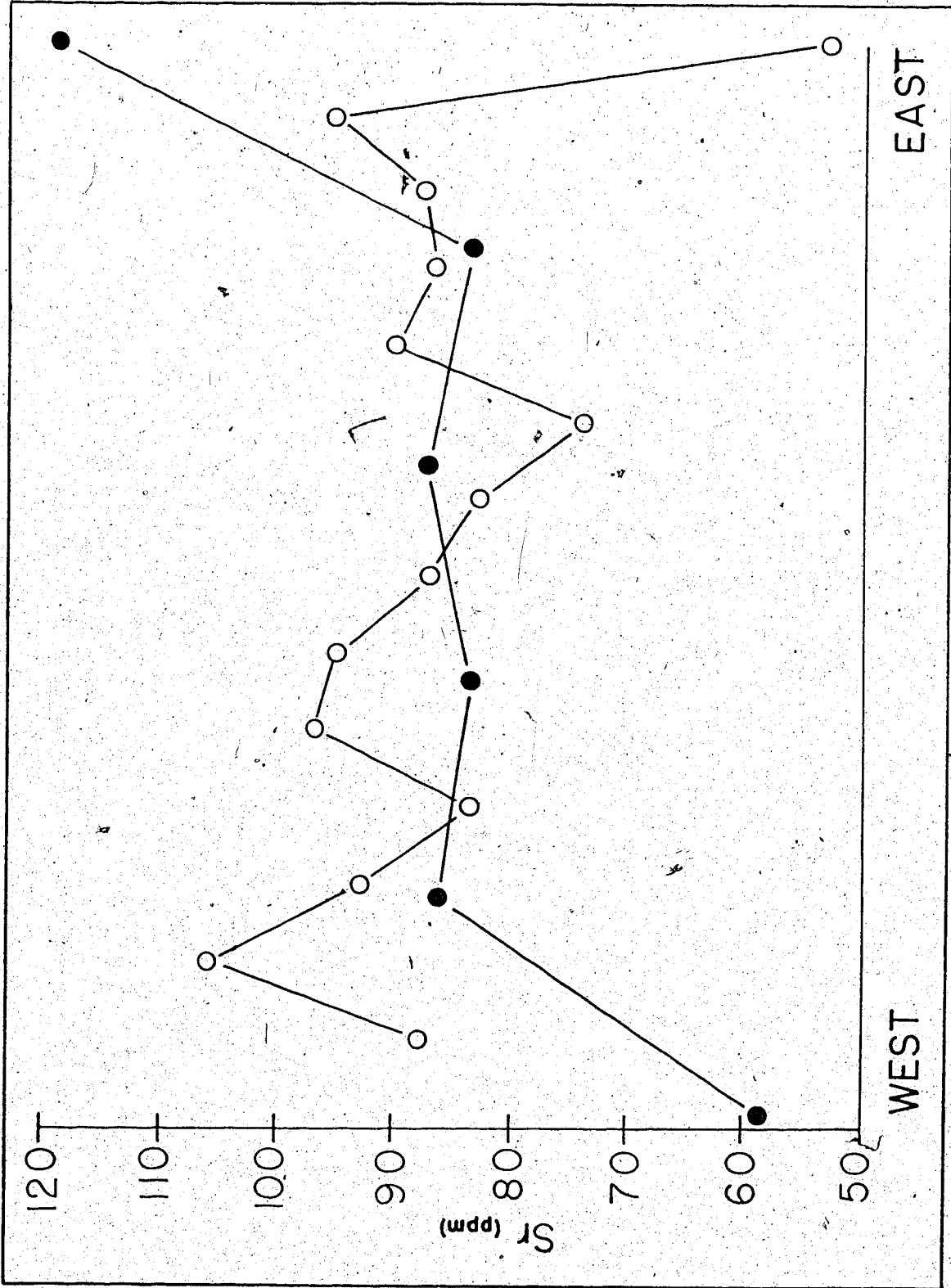


Figure 9: Sr concentrations in W-E traverses across Dyke I; open circles represent samples from the 292234 suite; closed circles, the 225952 suite.

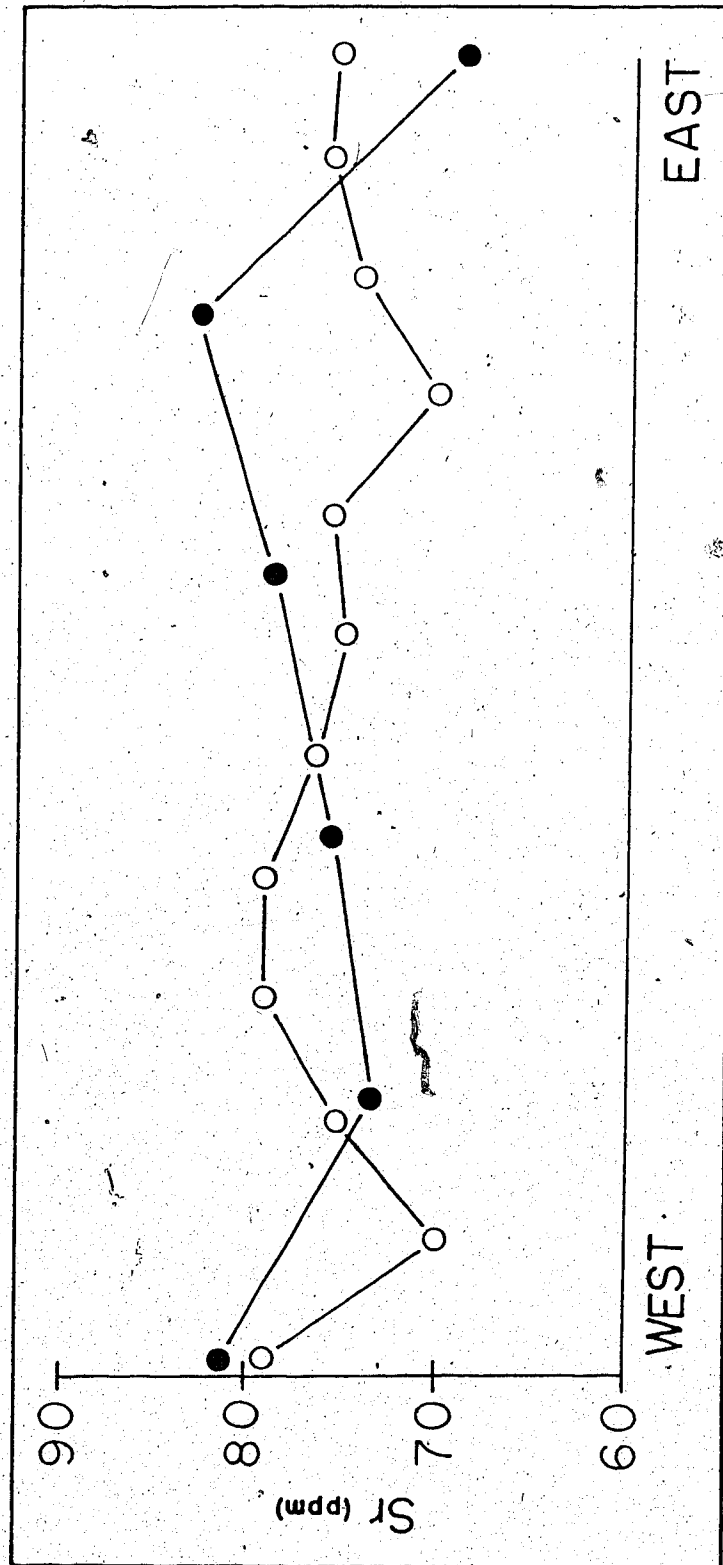


Figure 10: Sr concentrations in W-E traverses across Dyke II; open circles represent samples hosted by the gneisses; closed circles, the garbenschiefer.

samples which intrude the garbenschiefer unit of the supracrustals are on average only slightly enriched in total Sr compared to samples which intrude the Amitsoq gneisses. However, three samples analyzed from the garbenschiefer unit are markedly depleted in total Sr in comparison to the dykes themselves (Table 2). Within Dyke II, lateral variation is as prominent as the variation found along the dyke axis indicating variable Sr isotopic distribution throughout the dyke. Although there is sporadic epidote group mineral microveining of some of the samples, the presence of the microveining is not governed by the particular host lithology intruded by the dykes.

In chapter 3 it was noted that samples from Dyke I have been completely recrystallized, and significant mineralogical changes have been introduced, most noticeably the presence of scapolite. Scapolite, as shown by Shaw (1960a, b), may contain up to 0.15 weight percent Sr. Introduction of upwards of 35 percent scapolite in some of the recrystallized samples may well serve as the source for the additional Sr present. Samples which have been scapolitized show on average slightly elevated Sr concentrations over samples which are devoid of the mineral.

Rubidium concentrations are graphically displayed in the same manner as the Sr data in Figures 11 and 12. Rb shows a more regular behaviour, rarely exceeding 5 ppm whole rock concentration. Those samples which have high Rb concentrations contain elevated amounts of biotite. Displaying a pattern similar to the Sr, those portions of the dykes which intrude the supracrustals are enriched in Rb in relation to those hosted by the gneisses. The supracrustals for the most part are enriched above the dykes in Rb and depleted in Sr. The axial traverse along Dyke II displays slightly erratic behaviour in contrast to both margin to margin traverses across the dyke, this may in part correlate with the visible evidence of tectonic deformation of the dykes in certain localities.

Relative proportions of biotite increase in the sheared and foliated samples, indicating movement of an alkali rich fluid through the rock either during or after deformation had occurred. This is confirmed by the presence of elevated Rb values for samples displaying a tectonic fabric and increased amounts of biotite. No appreciable or comparative increase in Sr has been noted in these samples.

Scapolite again may assume a role in concentrating Rb. Shaw (1960a, b) calculated the average Rb concentration of 60 scapolite samples from around the world to be

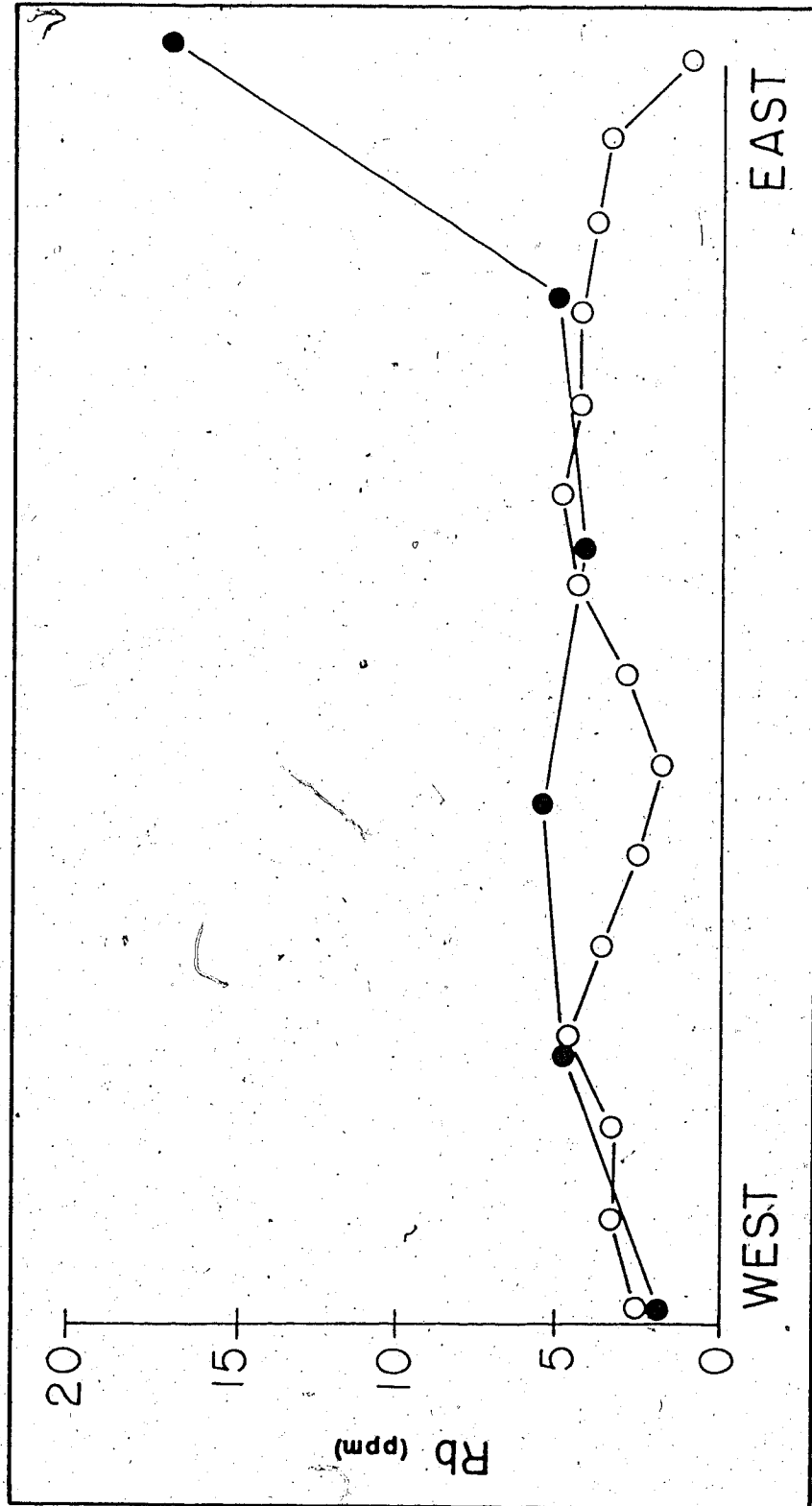


Figure 11: Rb concentrations in traverses across Dyke I; open circles represent samples from the 292234 suite; closed circles the 225952 suite.

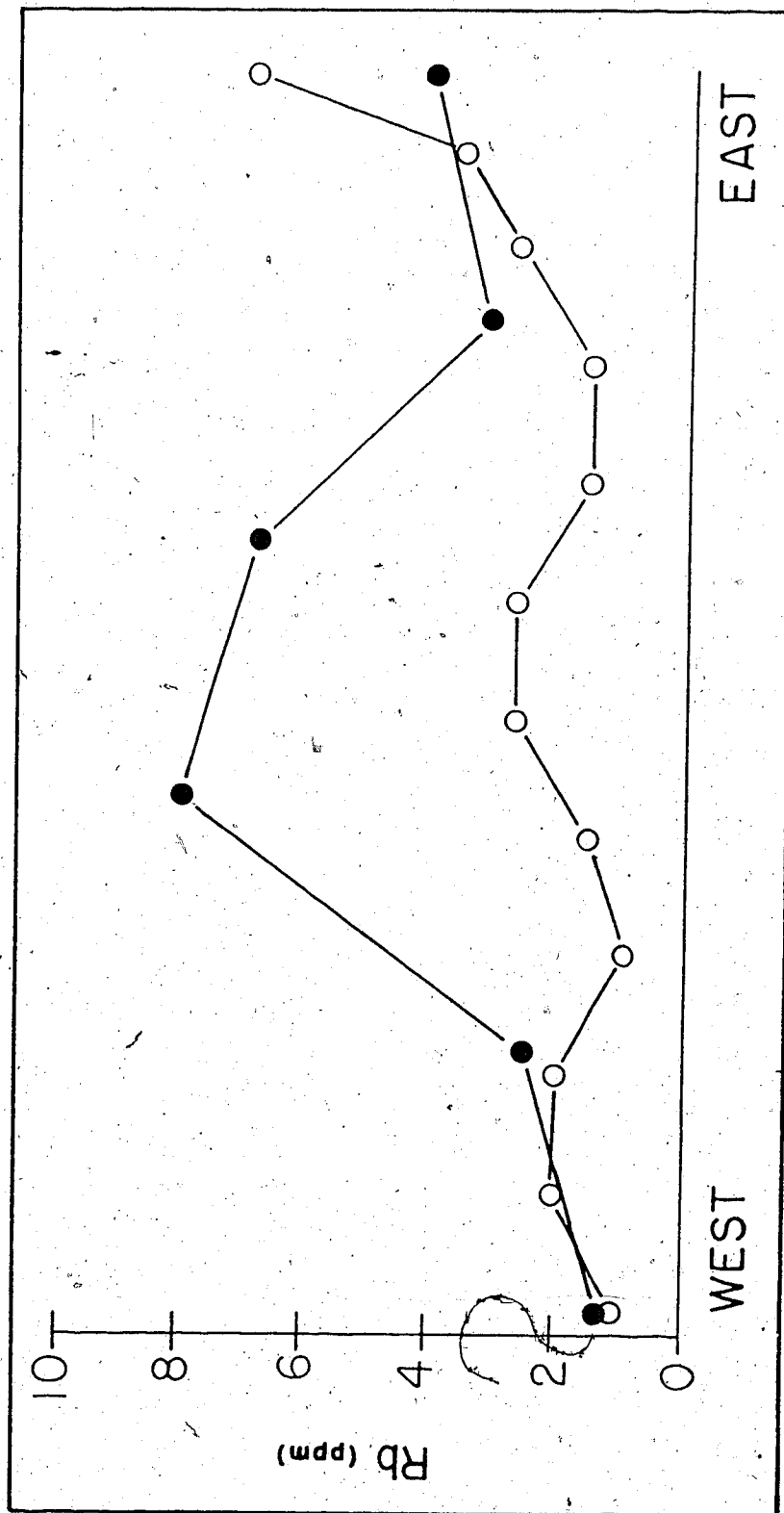


Figure 12: Rb concentrations in traverses across Dyke II; open circles represent samples hosted by the gneisses; closed circles, the garbenschiefer.

approximately 20 ppm, with concentrations ranging from 3 to 130 ppm. The average whole rock Rb concentrations of the Ameralik dykes is 2.51 ppm for dykes hosted by the Amitsoq gneisses and 3.22 ppm for samples showing no sign of scapolite and hosted by the garbenschiefer. The Rb concentration of those samples which have been scapolitized is nearly 5 ppm, representing nearly 100 percent enrichment of the dykes in Rb as compared to the unscapolitized dykes.

Clearly the distribution of whole rock Rb and Sr concentrations, scatter in measured isotopic ratios and calculated $^{87}\text{Sr}/^{87}\text{Rb}$ ratios demonstrate either incomplete homogenization of the dykes during the last metamorphic event, partial open system behaviour of the dykes or partial assimilation of pre-existing crustal material during emplacement.

B. Ameralik Dykes, Lead-Lead Results

Analytical results obtained on 100 whole rock samples are listed in Table 3 (Appendix I) and are presented in Figure 13. As with the Sr data, results from and within the dykes scatter too widely to produce an isochron. It is again necessary to examine the dykes individually and the trends which are presented by each. Samples which are characterized by highly radiogenic ratios are excluded from Figure 13. Only lead compositions believed to be more representative of primitive basalts have been utilized.

It is difficult to qualitatively discuss results obtained from the random dyke samples. Rb-Sr results have shown that these dykes are isotopically inhomogeneous as a group, despite apparent geochemical similarity (Gill and Bridgwater, 1979, p. 700). Lead results are no different. The scatter is wide and there is no apparent possible correlation with either dyke direction or degree of alteration. Data from Dykes I and II show somewhat more coherent behaviour with few notable exceptions. Dyke I leads appear to be more radiogenic than Dyke II.

The Pb-Pb results for Dyke II may be subdivided two distinct populations, corresponding to the host rock lithology. Samples from the dyke hosted by the garbenschiefer unit have the higher $^{207}\text{Pb}/^{206}\text{Pb}$ ratios while samples hosted by the Amitsoq gneisses have a lower ratio (Figure 14). Pb-Pb data points for samples from Dyke II display a weak, fan shaped distribution. If the system displayed linear data, two

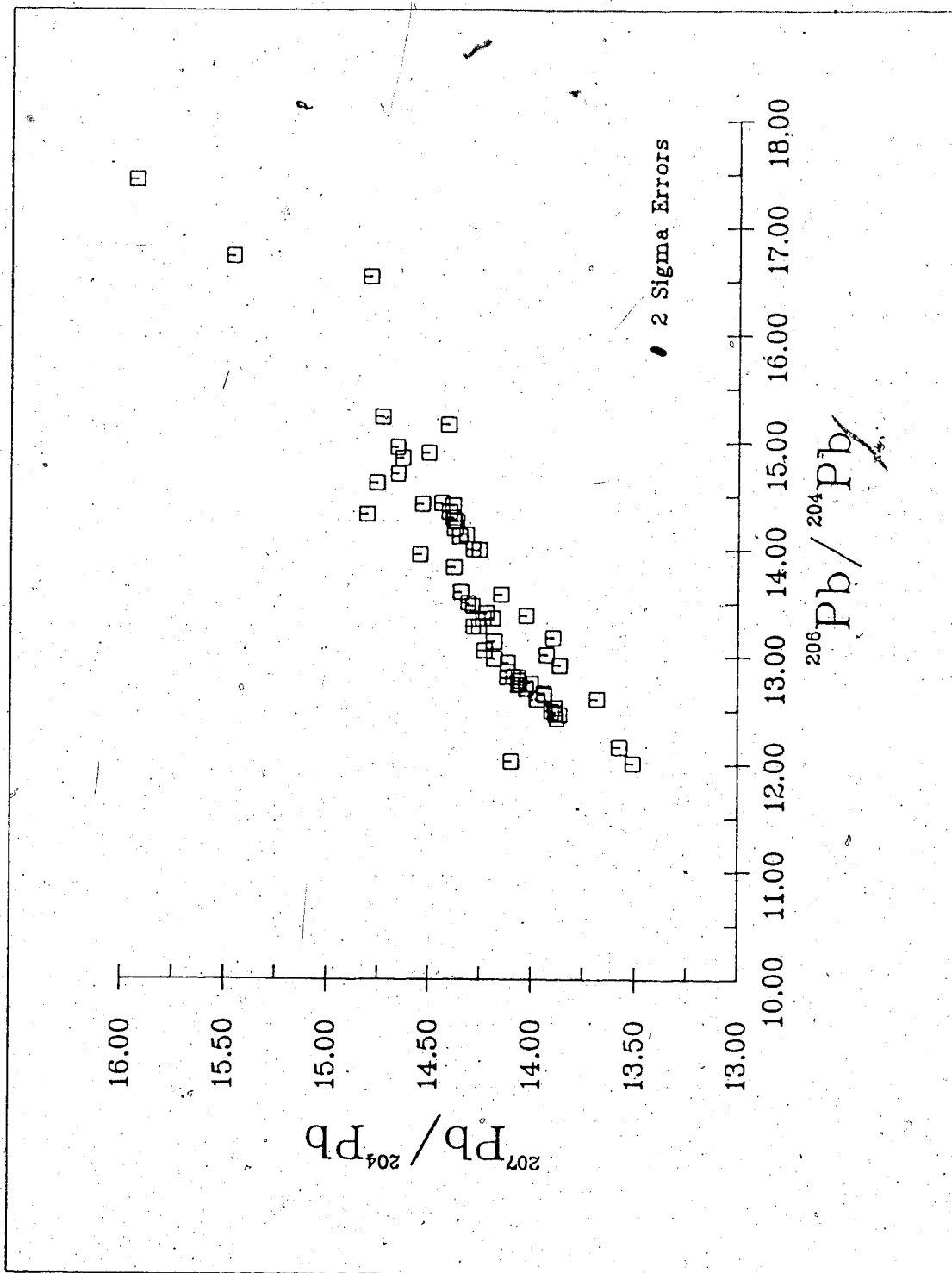


Figure 13: Plot of $^{207}\text{Pb}/^{204}\text{Pb}$ versus $^{206}\text{Pb}/^{204}\text{Pb}$ for whole rock Ameralik Dyke samples.

interpretations are possible. First, the magma has experienced no post-emplacment disturbance up to the present time, or the rock has been subjected to metamorphic conditions for a brief period of time, during which the rocks behaved as a closed system and were able to reach chemical and isotopic equilibrium. If the dyke rocks have been chemical open systems, lead and uranium are free to migrate into or away from the dykes. The resultant data will rarely display linear behaviour, since equilibrium in open chemical systems is difficult to obtain. Slope ages, calculated from the lower boundary of the scatter, may approach the age of the last metamorphic event giving the scattered distribution of the data points. Distribution of the data points about the 'apex' of the fan occasionally may indicate the time of the original formation.

Samples containing highly radiogenic $^{207}\text{Pb}/^{206}\text{Pb}$ ratios were eliminated from the data in an effort to evaluate lead systematics with presumably primitive samples. $^{207}\text{Pb}/^{206}\text{Pb}$ versus dyke position was calculated and plotted (Figure 14) to determine which samples (if any) define a region of high radiogenic values. In the recrystallized, scapolitized dyke samples, the margins show an increased radiogenic lead enrichment, becoming more primitive toward the dyke centre. The presence of allanite, a U, Th, REE bearing mineral of the epidote group, has been noted along the western margin. The dyke rocks reflect the presence of allanite by showing higher $^{208}\text{Pb}/^{204}\text{Pb}$ ratios (Table 3). Though no allanite has been described from the eastern margin of the dyke, it is assumed to be present since the eastern margin leads also have high $^{208}\text{Pb}/^{204}\text{Pb}$ ratios. If the $^{207}\text{Pb}/^{206}\text{Pb}$ for Dyke I cross-section is plotted versus position in the dyke, the centre portion of the dyke shows a very consistent ratio. This is likely an original feature of the dyke since secondary metamorphism would tend to act from the edge of the dyke toward the centre and would be variable. If the Dyke I samples with the same $^{207}\text{Pb}/^{206}\text{Pb}$ ratios (Figure 14) are selected for an isochron plot, a line is not obtained. This could simply be a result of widely scattered $^{207}\text{Pb}/^{204}\text{Pb}$ versus $^{206}\text{Pb}/^{204}\text{Pb}$ ratios. This may be a feature inherited from the initial dyke intrusion because of Pb contamination. Therefore the isotopic effect of the scapolitization on the Pb may be much less than that for Rb-Sr.

Isotope ratios calculated from Dyke II also show a distinctive pattern on a plot of $^{207}\text{Pb}/^{206}\text{Pb}$ versus dyke position (Figure 14). The overall $^{207}\text{Pb}/^{206}\text{Pb}$ ratios are almost 10 percent higher. Dyke II displays $^{207}\text{Pb}/^{206}\text{Pb}$ values of up to 1.1, compared to 1.0 and less

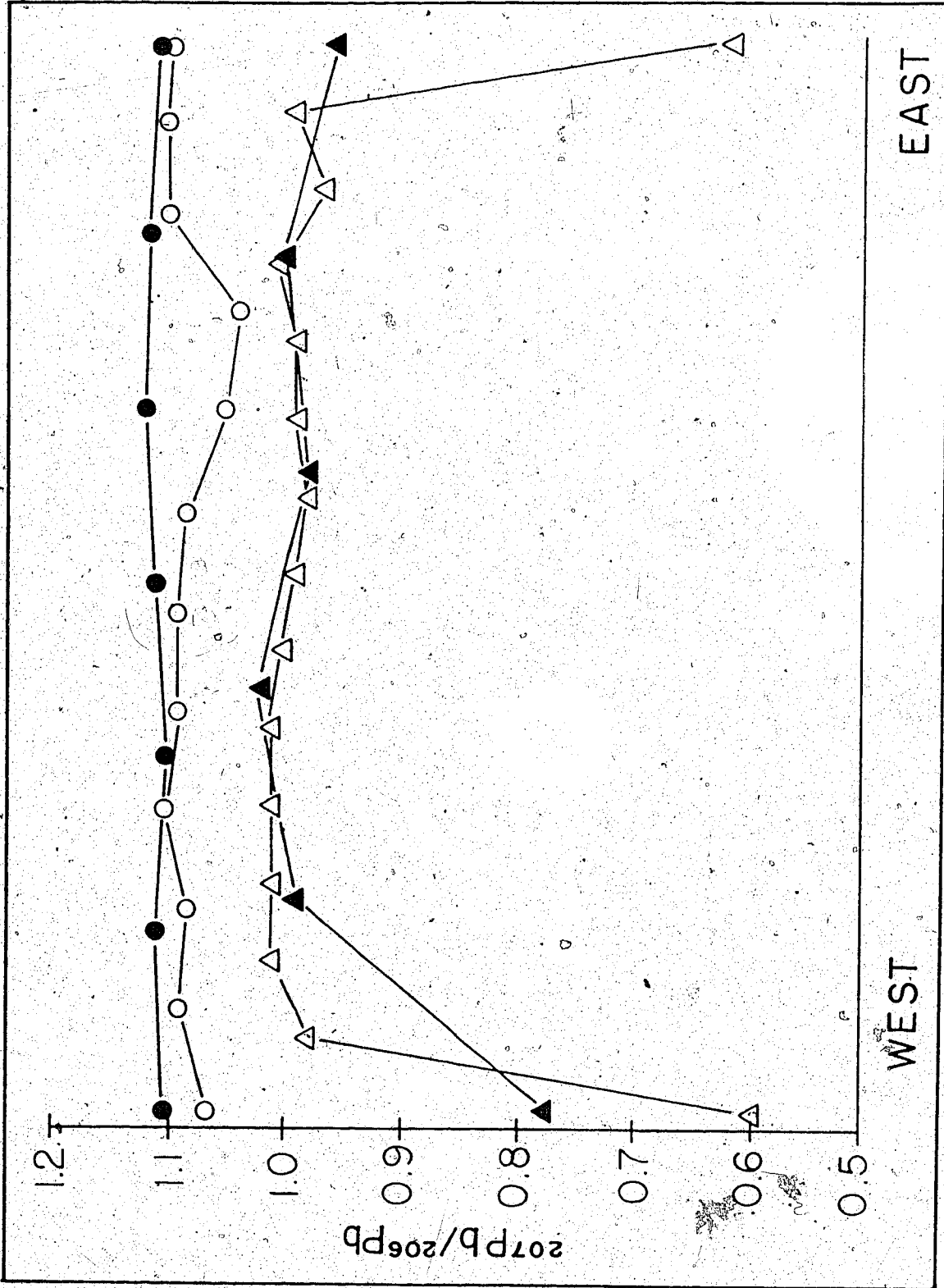


Figure 14: Plot of $^{207}\text{Pb}/^{206}\text{Pb}$ ratios for Dykes I and II; open circles represent samples hosted by the gneisses; closed circles, the garbenschiefer; open triangles, the 292234 suite; closed triangles, the 225952 suite.

for samples from Dyke I. Leads from Dyke II samples hosted by the supracrustals are marginally less radiogenic than leads from gneiss-hosted dykes. This is possible evidence for limited assimilation of pre-existing crustal material during emplacement. Fratta and Shaw (1974) have examined incompatible element (K, Rb, Li, Tl) concentrations in dykes from the Canadian shield to estimate amounts of 'residence contamination' possible by intrusion of basaltic magma into varying country rock. Their results are consistent with those obtained by Gates (1971), which indicate host rock contamination of primitive basaltic magma during emplacement is variable.

Three garbenschiefer samples analyzed (292229 V, W, AE; Table 3) have less radiogenic $^{207}\text{Pb}/^{204}\text{Pb}$ and $^{206}\text{Pb}/^{204}\text{Pb}$ ratios. If the source of variance in the lead ratios of the dykes was caused by simple residence contamination, one would expect the garbenschiefer samples to contribute older, less radiogenic lead to the dykes. The difference in the apparent age of the two host lithologies of the Ameralik dykes is less than 200 million years. The resultant change in the $^{207}\text{Pb}/^{206}\text{Pb}$ ratio is expected to be minimal (calculated to be 0.038), and any assimilation of leads from the host rocks would be expected to make little difference in the radiogenic nature of the leads. Results obtained from measurements on Dyke I are plotted in Figure 15. It is of interest to note that samples from the same dyke, collected no more than 100 metres apart, have such varying lead compositions, and actually plot as two separate populations. Data are plotted on conventional $^{207}\text{Pb}/^{204}\text{Pb}$ versus $^{206}\text{Pb}/^{204}\text{Pb}$ diagrams with the model lead growth curve of Stacey and Kramers (1975) used for reference. In the generation of their growth curve, Stacey and Kramers (1975) postulated that lead in the mantle grew from 4,570 Ma to approximately 3,700 Ma as a system with an initial μ ($^{238}\text{U}/^{204}\text{Pb}$) value of 7.18. At 3,700 Ma, there was a catastrophic change in the mantle μ value as it moved upwards to 9.74. This model is in direct contrast to the mantle evolution model of Cumming and Richards (1975), which postulates continual evolution of the mantle with a primordial μ value of 8.327.

Use of the Stacey and Kramers (1975) growth curve serves only as a first approximation to the true μ value of the source from which the Ameralik dykes were generated. Since uranium and thorium were not measured for this study, no direct measurement of the Ameralik μ is possible, but by making a series of assumptions, an

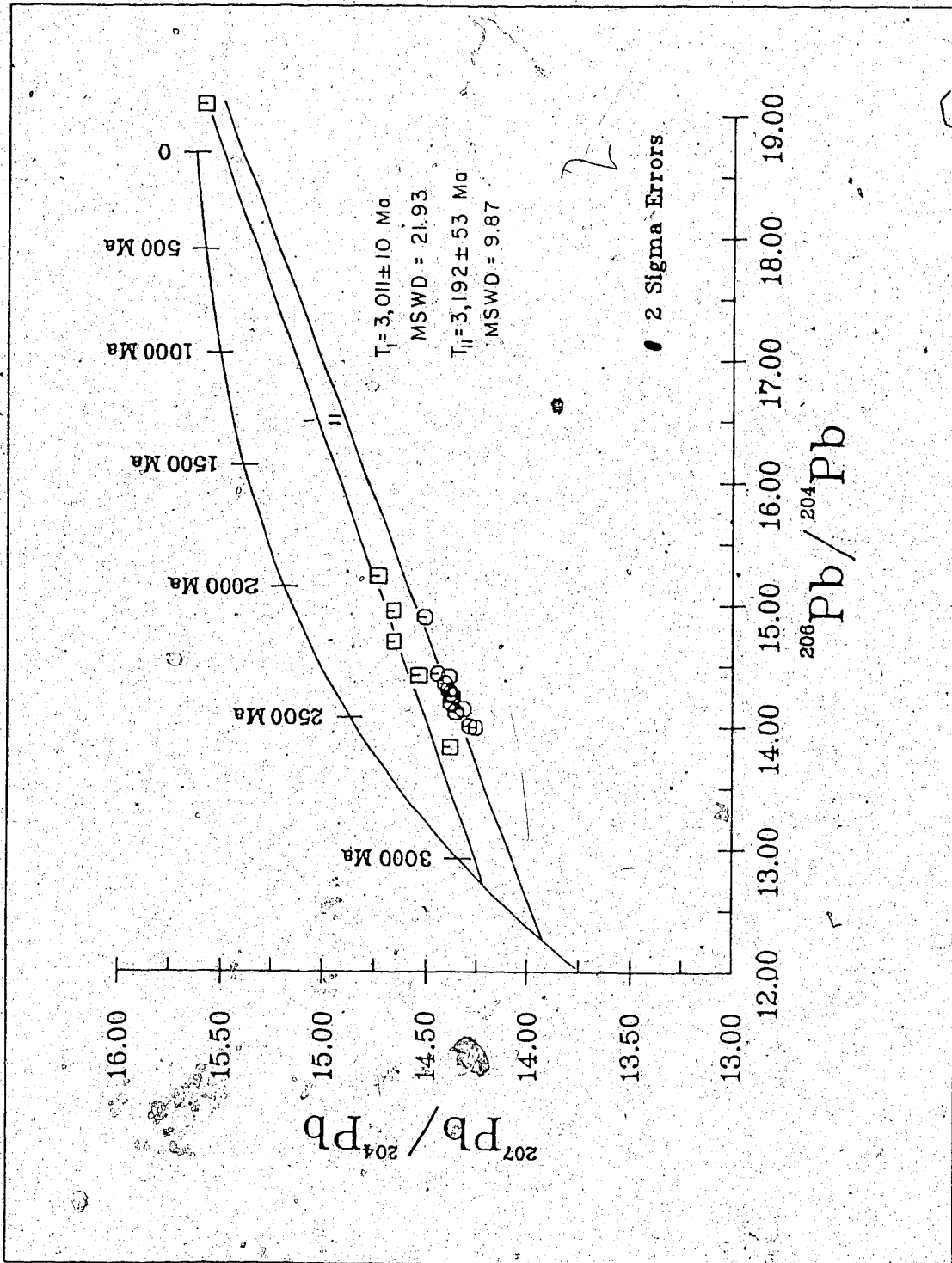


Figure 15: Plot of $^{207}\text{Pb}/^{204}\text{Pb}$ versus $^{206}\text{Pb}/^{204}\text{Pb}$ for W-E traverses across Dyke I; squares are samples from the 225952 suite; circles, the 292234 suite

approximate μ value for the dykes may be calculated.

It is known that the Ameralik dykes lie between 3,100 and 3,600 Ma based on field relationships (see Table 2). Utilizing the Holmes-Houtermans (1946) model lead age calculation equations, 3,600 Ma as the older age limit and 3,100 Ma as the younger age limit in the general equation:

$$(^{206}\text{Pb}/^{204}\text{Pb})_t = (^{206}\text{Pb}/^{204}\text{Pb})_0 + \mu((\exp)\lambda T - (\exp)\lambda t) \text{ where:}$$

λ is the ^{238}U decay constant ($1.55125 \times 10^{-10} \text{ yr}^{-1}$) (Jaffey *et al.*, 1971)

$$(^{206}\text{Pb}/^{204}\text{Pb})_0 = 9.307 \text{ (Tatsumoto } et al., 1973).$$

Using these values, it is calculated that μ values for the Ameralik dyke system average approximately 7.52, assuming single stage growth of the parent system.

Utilizing the μ values calculated for the dykes to generate a common lead growth curve, intersection ages of the dykes have been computed as follows:

Dyke I, initial sample collection, $3,011 \pm 10$ Ma, MSWD = 21.93

Dyke I, follow-up collection, $3,192 \pm 53$ Ma, MSWD = 9.87

Dyke II, E-W traverse, gneissic host, $3,157 \pm 57$ Ma, MSWD = 7.96

Dyke II, E-W traverse, garbenschiefer host, $3,306 \pm 63$ Ma, MSWD = 6.18

Dyke II, dyke centre samples, $3,044 \pm 228$ Ma, MSWD = 256.03

Dyke II, composite, $3,209 \pm 77$ Ma, MSWD = 35.05

These are in variable agreement with the corresponding calculated slope ages of:

Dyke I, initial sample collection, $3,222 \pm 39$ Ma, MSWD = 13.92

Dyke I, follow-up collection, $3,248 \pm 59$ Ma, MSWD = 8.97

Dyke II, E-W traverse, gneissic host, $3,823 \pm 12$, MSWD = 7.86

Dyke II, E-W traverse, garbenschiefer host, $3,938 \pm 118$, MSWD = 12.36

Dyke II, dyke centre samples, $3,860 \pm 18$ Ma, MSWD = 199.36

Dyke II, composite, $3,929 \pm 16$ Ma, MSWD = 71.75

Examination of data obtained suggest that the very old slope ages are due to addition of variable quantities of less radiogenic lead supplied by the host rocks which have significantly altered the primary lead isotopic composition of the dykes. If the results obtained from the original collection of samples from Dyke I are eliminated, the calculated and computed ages lie within error of each other, possibly indicating the true age of emplacement of the Ameralik dyke swarm.

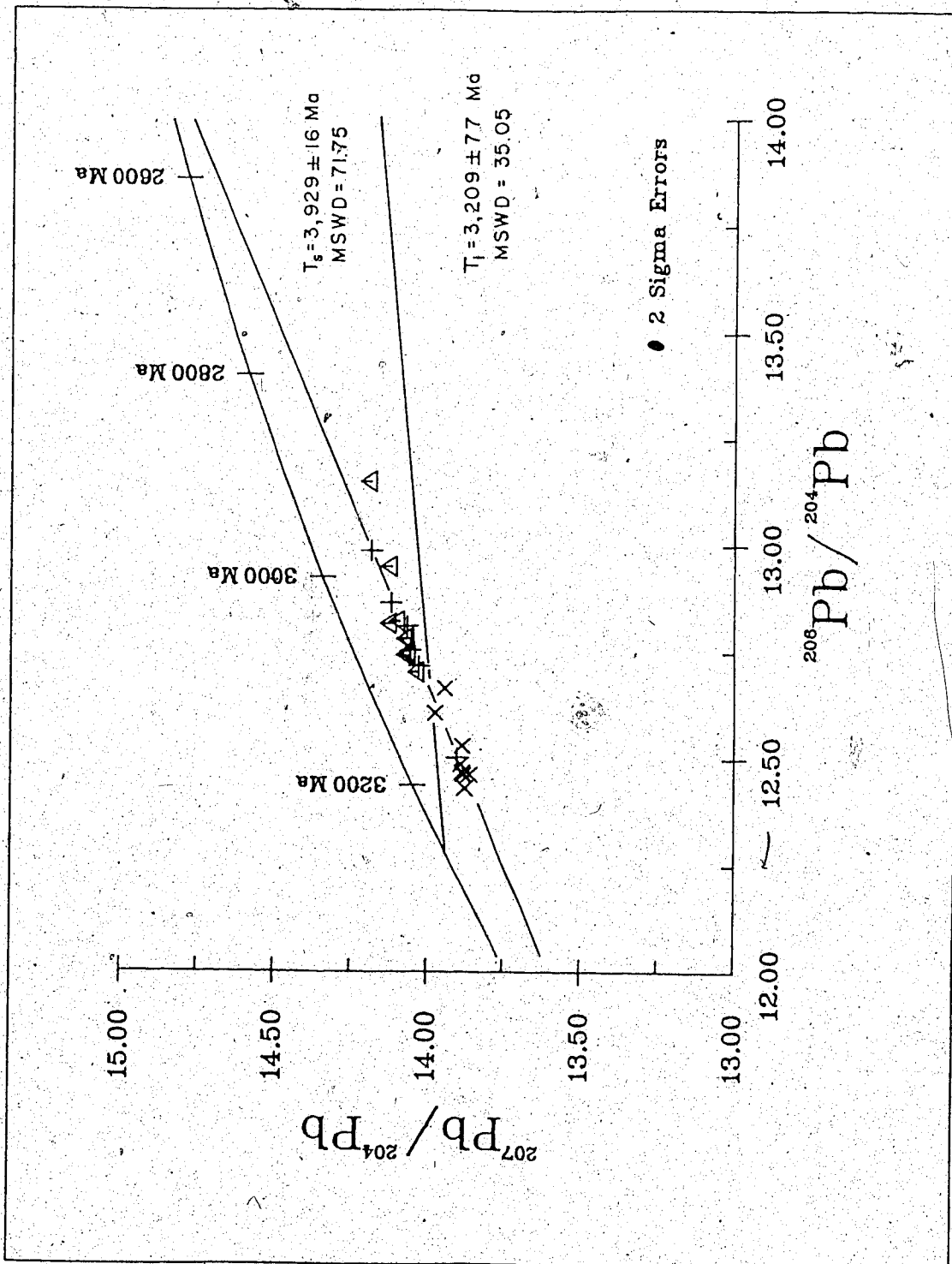


Figure 16: Plot of $^{207}\text{Pb}/^{204}\text{Pb}$ versus $^{206}\text{Pb}/^{204}\text{Pb}$ for traverses across and along Dyke II; crosses are garbenschiefer hosted samples; triangles, gneiss hosted samples; pluses, axial traverse.

C. Proterozoic Dyke III, Rubidium-Strontium and Lead-Lead results

Results obtained from both Rb-Sr and Pb-Pb analyses for a large Proterozoic dyke (Dyke III) are listed in Tables 4 and 5 (Appendix I) and shown in Figures 17 and 18. Data points from Rb-Sr and Pb analyses again exhibit widespread scattering on data plots and variable isotopic values across and along the dyke. This is graphically displayed in Figure 19, which treats the data for Dyke III in the same manner as that for the Ameralik dykes I and II.

Neither Rb, Sr nor Pb display systematic behaviour within the dyke. Dyke III is the only dyke which does not conform to the geologic structure of the host garbenschiefer. It partly intrudes rocks of the calc-silicate and upper ironstone formations (Figure 6), pinching and swelling along its length (H. Baadsgaard, pers. comm.) and intruding the tectonically deformed gneissic terrane to the south of the Isua supracrustal belt.

Although the sampled portion of the dyke lies entirely within the garbenschiefer unit of the supracrustals, in certain sample locations along the line of traverse, the dyke is in contact with the ironstone formation. This apparently does not affect the isotopic composition of the rocks.

Erratic Rb, Sr and $^{207}\text{Pb}/^{206}\text{Pb}$ distribution patterns indicate possible isotopic contamination from one or more sources. Behaviour of Rb and Sr show that chemical differentiation during cooling of the parent magma is not solely responsible for the observed patterns. If it were, Rb should systematically increase toward the dyke centre and remain essentially constant along its length. Sr might be expected to concentrate closer toward the dyke margin (cf. Gill and Bridgwater, 1979). Neither pattern displayed suggests this type of chemical behaviour is present in Dyke III.

Deuteric alteration is present in the form of saussuritic feldspars and uralitic pyroxenes. Variable amounts of alteration seen from sample to sample may serve as one cause of isotopic variability within the dyke.

Comparison of data from Dyke III with that for Dykes I and II reveals differences in behaviour of the isotopes, chemical composition, mineralogy and style of intrusion (the cross-cutting of all local features). It is of interest to note the results obtained from isotopic analyses, especially Pb-Pb results, indicate continuity of development and extension of isotopic patterns displayed by the Ameralik dykes (Figures 15, 16 and 18).

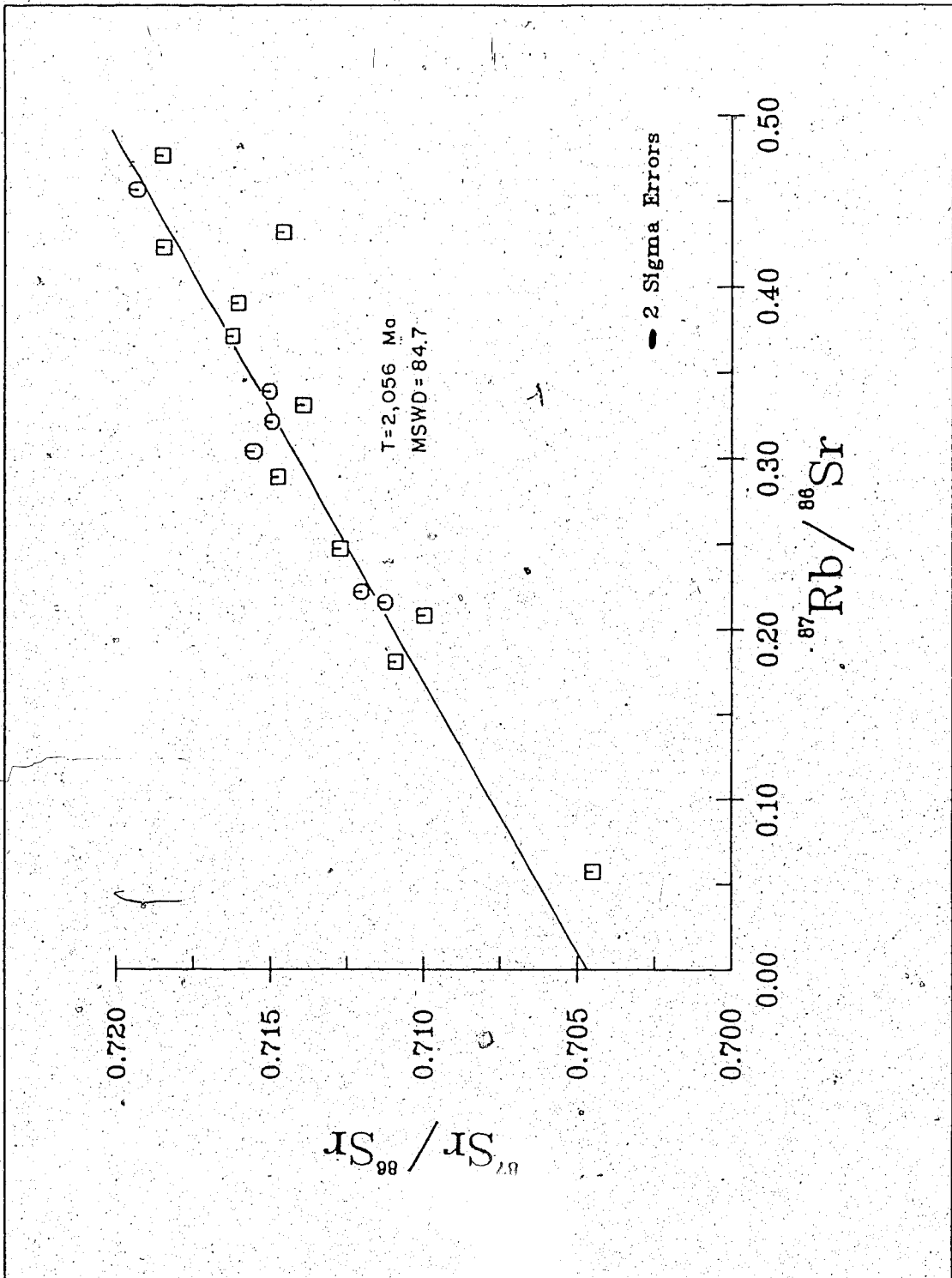


Figure 17: Plot of $^{87}\text{Sr}/^{86}\text{Sr}$ versus $^{87}\text{Rb}/^{86}\text{Sr}$ ratios for the Proterozoic Dyke; squares, W-E traverse; circles, axial traverse.

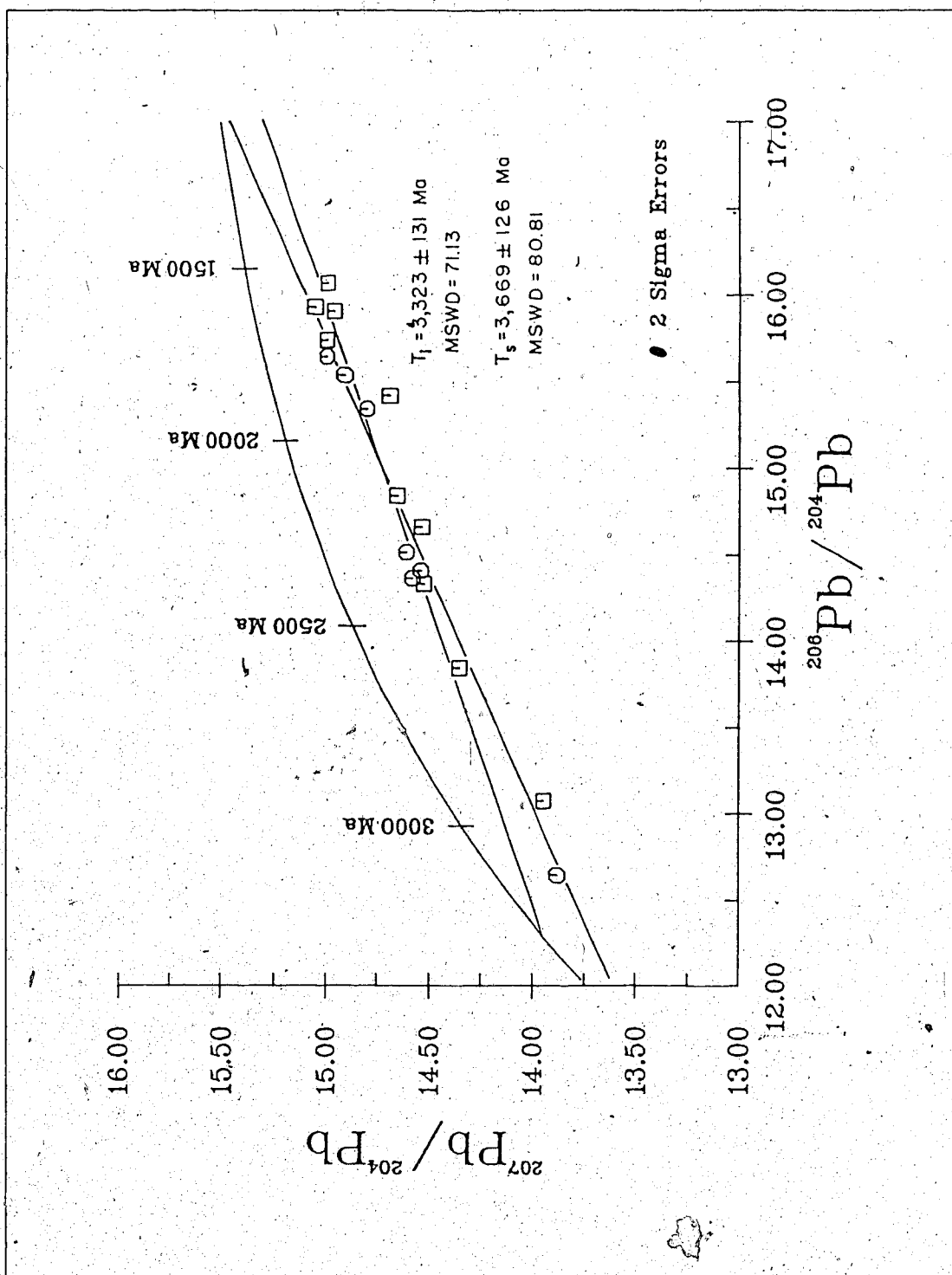


Figure 18: Plot of $^{207}\text{Pb}/^{204}\text{Pb}$ versus $^{206}\text{Pb}/^{204}\text{Pb}$ ratios for the Proterozoic dyke; squares, W-E traverse; circles, axial traverse.

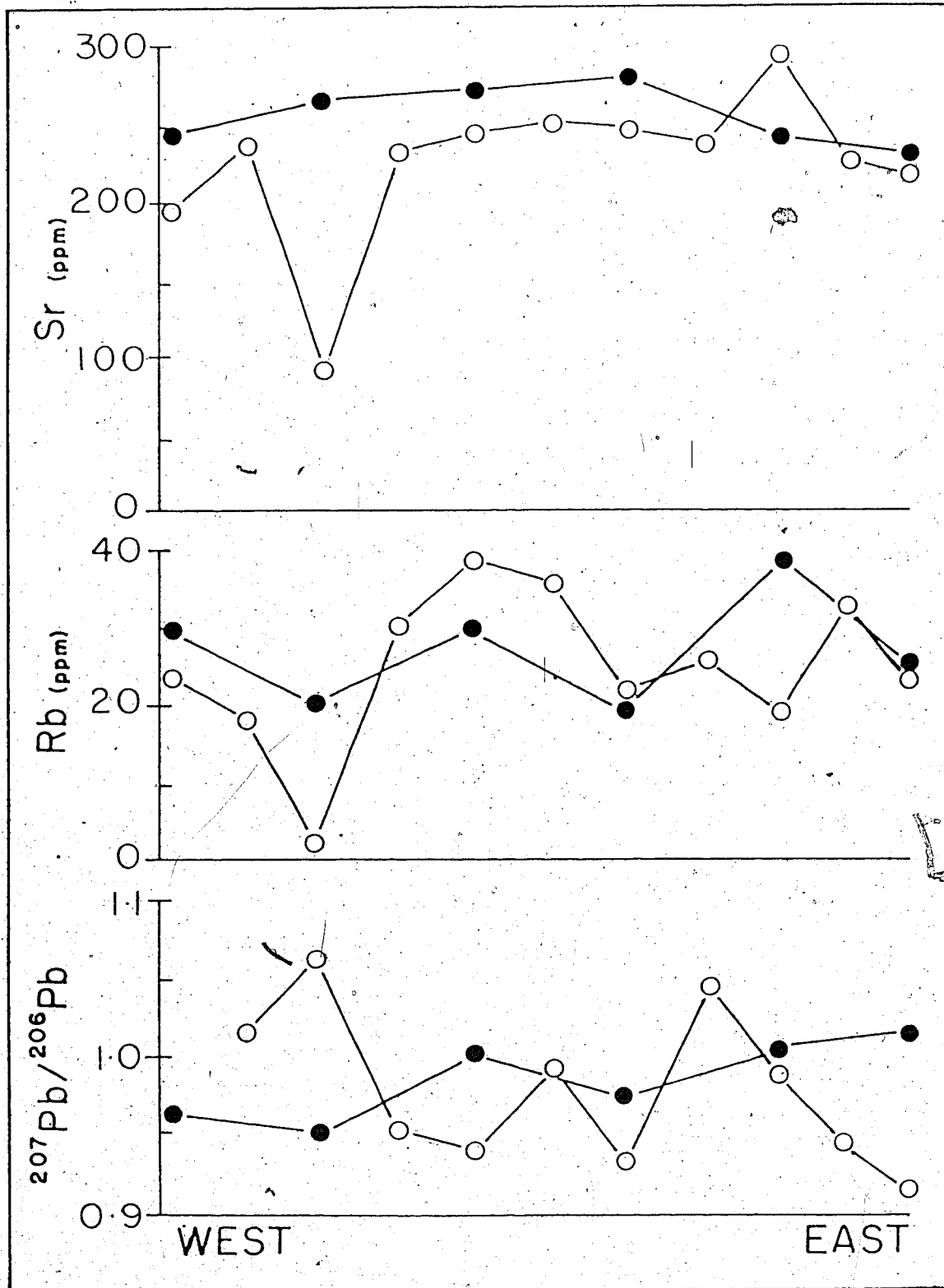


Figure 19: Variations in Sr, Rb and $^{207}\text{Pb}/^{206}\text{Pb}$ in traverses across the Proterozoic dyke; open circles represent the W-E traverse; filled circles, the axial traverse.

If data from Pb-Pb analyses obtained from Dyke III are treated in similar fashion to that from Dykes I and II, the following results are obtained from growth curve intercept ages:

Dyke III, E-W traverse, $3,356 \pm 189$ Ma, MSWD = 73.62

Dyke III, dyke centre samples, $3,101 \pm 217$ Ma, MSWD = 26.97

Dyke III, composite, $3,323 \pm 131$ Ma, MSWD = 71.13

and the calculated slope ages:

Dyke III, E-W traverse, $3,670 \pm 20$ Ma, MSWD = 92.02

Dyke III, dyke centre samples, $3,726 \pm 13$ Ma, MSWD = 37.71

Dyke III, composite, $3,669 \pm 126$ Ma, MSWD = 80.81

As with Dyke II, the calculated slope age is much older than the computed growth curve intercept age, again suggesting the likelihood of assimilation of contaminant lead from the host rock, altering the original lead isotopic composition of the magma.

Since there are no geological features which place older and younger age limits upon Dyke III, it is difficult not to associate it with the Ameralik dykes solely based upon Rb-Sr and Pb-Pb data obtained here.

Samples taken from along the axis of Dyke III do not display uniform isotopic behaviour, though there is more regularity in the values. Scatter among the data, though not variable to the same degree as those taken across the dyke, is present and cannot be explained in the context of chemical differentiation. Possible reasons for the variance of elemental concentrations and isotopic ratios are similar to those discussed for the Ameralik dykes, except here petrological analysis reveals no evidence for recrystallization for the dyke nor for the migration of any alkali bearing fluids. Clearly, geological processes associated with emplacement and deuteric alteration are implicated here as the major source of the variations found within Dyke III.

VI. INTERPRETATION AND CONCLUSIONS

A. Interpretation of the Results

Data presented in the previous chapter show clearly that certain elemental distribution patterns within the individual dykes developed as a result of the modification of the primary magmatic composition. These processes could have occurred during or after emplacement. It is possible that combined effects of several processes may help to explain the scattered results.

Studies of chemical (Fratta and Shaw, 1973; Dostal and Fratta, 1977) and isotopic (Patchett *et al.*, 1979; Patchett, 1980) modification (during emplacement) of doleritic dykes have brought attention to the effects of post-magmatic hydrothermal fluids and the possibility of contamination by related processes. The recognition of these alteration effects, and the distinction between primary (during emplacement) and secondary (metamorphic, metasomatic) chemical and isotopic patterns are of utmost importance in the interpretation of the geochronology of doleritic bodies such as the Ameralik dykes.

Models to be examined here include residence contamination, alkali metasomatism and assimilation of pre-existing crustal material.

The phenomenon of residence contamination is a process whereby magma interacts with wall rocks during emplacement. The interaction is in response to the presence of chemical potential gradients. The process occurs either through fluid induced grain boundary diffusion, or in the case of still molten magma, through volume diffusion along compositional gradients between wall rock and magma (Fisher and Lasaga, 1981). Gates (1971) and Fratta and Shaw (1973) have illustrated that selective contamination by K and Rb in Proterozoic dykes from the Canadian Shield occurred prior to final crystallization of the magma. Some question remains as to whether alteration of, and elemental enrichment of the dykes are primary or secondary. Element distribution patterns presented in both studies suggest primary emplacement contamination, with the possibility of some deuteric alteration.

Data patterns obtained from Ameralik dyke samples deviate from those presented by Gates (1971), more closely approximating those of Fratta and Shaw (1973). The erratic behaviour of alkalis here is attributed to diffusion and differentiation processes

active during crystallization of the magma. One outstanding difference which may lessen the overall importance of residence contamination as a possible single source model for isotopic variation, is the response of the dykes to intrusion through different host rocks. The Ontario samples (Gates, 1971; Fratta and Shaw, 1973) show that dykes have higher Rb when intruding granitic country rocks than when they occur in basic volcanics. At Isua the opposite is apparently true. Samples intruding the Amitsoq gneisses appear depleted in Rb in relation to samples hosted by the garbenschiefer. When surrounded by the garbenschiefer, the dyke momentarily conforms to the local structure of the host rock. These rocks may be slightly more deformed than their gneissic counterparts, thus allowing easier migration of hydrothermal fluids. Enrichment of radiogenic Sr is variable and is possibly a function of the amount of epidote group mineralization present. Radiogenic Sr tends to accumulate in Ca rich alteration phases associated with deuteric hydrothermal fluid migration.

Scapolitized samples are not included in this discussion due to the obvious alteration which serves to mask effects of primary contamination. Work by Gill and Bridgwater (1976, 1979) has demonstrated residence contamination is present in the Ameralik dykes, though the effects of such contamination appear to be restricted primarily to the dyke margins. Such a claim is not easily established on whole rock Rb and Sr concentrations obtained during this study. Gates (1971) has suggested a possible reason for the discord is selective cation leaching from the country rock by late stage deuteric fluids from the intruding dolerite. Thus while there may have been some limited exchange of mobile cations (residence contamination), the results presented herein do not allow this to be the sole cause of the isotopic variations found in the dykes.

Alkali metasomatism entails a change in whole rock mineralogy and chemistry caused by migration of alkali-bearing fluids. Alteration mechanisms are similar in nature to those caused by skarn formation, which may be either local or widespread. Petrographic and geochemical evidence from the Ameralik dykes suggest limited post-emplacement migration of alkalis. Variable K/Rb ratios measured in the dykes (Gill and Bridgwater, 1979) and the presence of alkali amphibole (arfvedsonite?) encrusting granular aggregates of amphiboles (Plate 8) are the strongest evidence available. Limited appearance of biotite replacing either amphibole or sphene (Plate 6) also suggests some alkali diffusion. Host

rock lithology may be important. Mineralogical and textural changes caused in the dykes by metasomatic processes are likely to be minimal at the dyke centre. Gill and Bridgwater (1979, Table 5) have demonstrated a dependence of elemental migration on host rock lithology and sample position within the respective dykes. Supracrustal hosted samples show increase in CO_2 toward the dyke margin while Ca and K remain essentially unchanged. Thus Rb seems likely also to be unaffected. For those dyke samples which are unscapolitized, this apparently holds true (cf. Figure 14). CO_2 and Ca show depletion nearer the dyke margins whereas K and Rb increase. Positive proof of alkali migration and associated alteration must be derived from petrographic examination of the dykes. In all but a few samples, biotite is completely absent from the dykes. Whole rock Rb concentrations average less than 5 ppm, but are as high as 105 ppm. Associated increases in $^{87}\text{Sr}/^{86}\text{Sr}$ are present in the high Rb samples. Not all dykes examined show traces of biotite or alkali amphibole. Recrystallized dykes (Dyke III included) show no indication of alkali migration. Alteration is very limited, and absent in most instances. It is suggested here, without benefit of microprobe data on the feldspars or mafic minerals, the presence of alkali amphibole results from degradation of the plagioclase feldspars. Limited to moderate saussuritic alteration of the feldspars, is evident in all specimens.

On the basis of the evidence presented, if alkali metasomatism was the predominant alteration process active during migration of deuteritic fluids, it is expected that increased amounts of K^+ and Rb^+ should be present. Positive evidence would include the presence of biotite and antiperthitic exsolution in the plagioclase feldspars. Little, if any of the above mentioned minerals are found in the dykes.

It is therefore concluded that, in respect to inferring alkali metasomatism to be the sole mechanism for isotopic variation found in the Ameralik dykes, such a process has not contributed significant amounts of any nuclides of interest to the dykes and is not responsible for the observed isotopic variations.

The final model to be examined is that of assimilation of pre-existing crustal material during emplacement of the primary magma. Several factors are important. McGregor (1973) and Gill and Bridgwater (1976) have postulated that the Ameralik dykes may have been emplaced into still warm country rocks, consistent with the model of Wells (1976) that present day surfaces at Isua have been exposed after erosion of 25 to

35 kilometres of overlying rock. Emplacement of the magma into warm country rock may easily have facilitated varying degrees of assimilation. Partial anatexis and remobilization of the host rock is possible at these elevated temperatures.

Variations in the degree of assimilation of crustal material have been recorded from many locations. A noteworthy example of isotopic contamination is displayed in Tertiary intrusives from the Isle of Skye, Northwest Scotland (Moorbath and Bell, 1965; Moorbath and Welke, 1969; Dickin, 1981). Pb and Sr isotopic investigations from Skye have shown that from 10 to 80 percent of the contained isotopes are derived from pre-existing crustal materials (in this case, chiefly Lewisian basement). Acidic rocks from Skye contain the largest component of remobilized crust. The mafic and ultramafic intrusives, while definitely contaminated, have assimilated a much smaller proportion of the basement complex during intrusion. The results from Skye point out the importance of the presence of underlying, older crust with relatively low U/Pb and high Rb/Sr ratios compared to values obtained from the upper mantle. The degree of assimilation is outlined on a model lead growth curve (Moorbath and Welke, 1969, Figure 3). All lead analyses lie on a secondary isochron, intersecting the growth curve at 2,900 Ma and 60 Ma respectively. The lead line represents classical two component mixing, allowing the authors to estimate relative amounts of contamination encountered in the rocks.

Recent investigations into the geochemistry of basalts from Skye (Moorbath and Thompson, 1980; Dickin, 1981; Thompson, 1982) suggest that variance in the isotopic compositions of the magmas resulted from one of several processes; magmatic equilibration in various parts of the upper crust coincident with fractional crystallization and silic contamination; selective Pb equilibration in a vapour or non-silicate phase between the magma and the Archaean sial, or in which the mantle derived magma contained fairly constant Pb, and the increasing degree of isotopic contamination was caused by greater additions of crustal Pb to the magma (selective magma-crust interaction). Sr data accumulated by Moorbath and Thompson (1980) indicate contamination of the basic magmas resulted from interaction between the melt and a Sr rich, ⁸⁷Sr rich crust as the magma fractionated in near surface magma reservoirs.

The obvious complexity in the genesis and emplacement of rocks at Skye serves to point out that extensive isotopic and geochemical investigations are required to

completely understand the generation and subsequent history of the generation of basaltic magmas in the Archaean, specifically at Isua.

Gates (1971) has also reported effects of crustal contamination on isotope ratios in late Archaean, early Proterozoic dykes from Ontario, Canada.

Two studies of large granitic and quartzo-feldspathic gneiss complexes near the Isua-Godthaabsfjord have been reported (Taylor *et al.*, 1980; Moorbath *et al.*, 1981). The ca. 3,050 Ma Nuk gneiss and the ca. 2,500 Ma Qorqut Granite have revealed marked enrichment of older, less radiogenic lead, brought in with the magma during emplacement by anatexis of underlying granitic crust.

The variable lead data obtained from the Ameralik dykes, both scapolitized and unscapolitized, may be treated as a result of a mixing contamination process. This is schematically represented in Figure 20. Field constraints place the younger limit for age of emplacement of the Ameralik dykes at the age of the Nuk gneisses, which has been measured at approximately 3,100 Ma. The older limit is set at the last recorded Archaean event to affect the Amitsoq gneisses approximately 3,600 Ma. The Stacey and Kramers (1975) model lead growth curve is used here as an approximation of μ at the time of emplacement of the Nuk gneisses (approx. $\mu = 7.5$). Several trends are immediately apparent upon examination of the data. With the exception of some data from the gneiss-hosted portion of Dyke II, none of the data lie on the 3,100 Ma secondary isochron, but well below. The lower secondary isochron is taken to represent composition of leads removed from the Amitsoq gneiss at approximately 3,100 Ma, developing undisturbed since that time. Data from the garbenschiefer-hosted, unscapolitized dykes lie near the Amitsoq-Nuk mixing line, the least radiogenic leads here may approximate the Pb isotopic composition of the primary magma, given that three analyses on the garbenschiefer itself lie within the lower cluster of points.

If assimilation of pre-existing crustal material is the major cause of isotopic heterogeneity in the unrecrystallized Ameralik dykes, the lead data suggests assimilation of 10 to 15 percent older crustal material during emplacement. The difference in the nature of the leads assimilated from their different host rocks are difficult to explain, but first approximations indicate Pb evolution occurred in regions of slightly different μ values for the garbenschiefer and the gneisses. Data from the Amitsoq gneiss studies

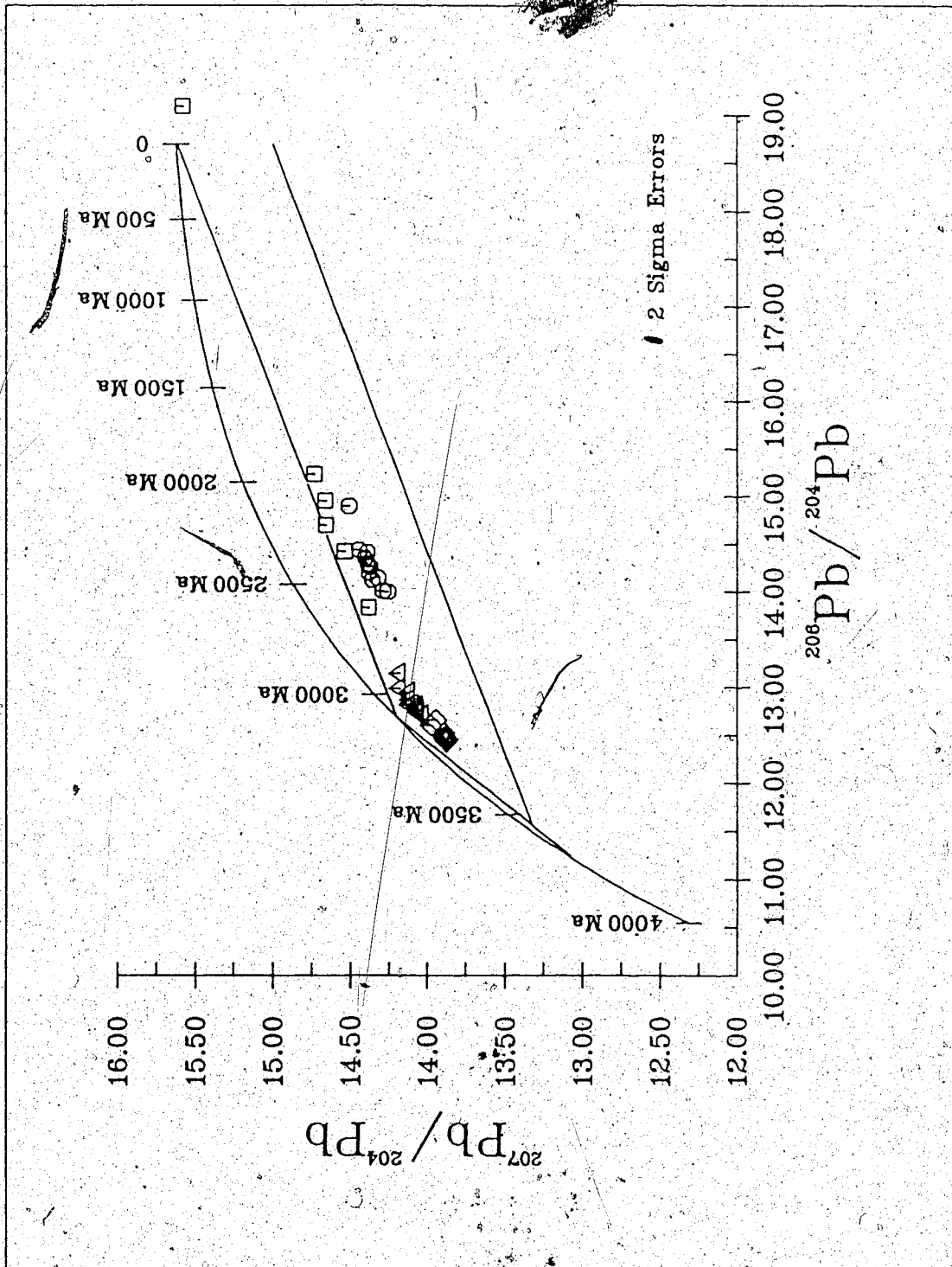


Figure 20: Plot of $^{207}\text{Pb}/^{204}\text{Pb}$ versus $^{206}\text{Pb}/^{204}\text{Pb}$ for Ameralik dykes showing assimilation of older, less radiogenic lead: Squares, 225952 suite; circles, 292234 suite; triangles, Dyke II, gneiss hosted samples; diamonds, Dyke II, garbenschiefer hosted samples.

(Baadsgaard 1973, 1976) indicate the gneisses evolved in a uranium depleted region. Evidence for similar development of the garbenschiefer unit is consistent with this model. Certain Ameralik dyke samples have shown strong depletion of uranium and have not been included in this portion of the discussion.

Data from the scapolitized samples (Dyke I) indicate input of a slightly more radiogenic lead component during recrystallization. The dyke was not completely rehomogenized during the event (shown by the lead data obtained from the separate dyke traverses). Incomplete homogenization of the isotopes within this dyke is exemplified by Rb/Sr data obtained on the original six samples (225952A-F) yielding an apparent Rb/Sr isochron slope age of $1,575 \pm 29$ Ma, MSWD = 0.79 and $(^{87}\text{Sr}/^{86}\text{Sr})_0 = 0.70512 \pm 0.00008$, whereas samples 100 metres distant failed to yield a similar isochron for $^{87}\text{Sr}/^{86}\text{Sr}$ versus $^{87}\text{Rb}/^{86}\text{Sr}$ ratios. The data here lead to the suggestion that scapolitization and recrystallization of this particular dyke, associated with the partial rehomogenization of the Rb/Sr isotope systematics occurred at approximately 1,575 Ma. This date is not unknown from work on the Amitsoq gneisses outside the Isua area (Bridgwater *et al.*, 1976). It is conceivable that the supracrustal belt, on the western margin of the gneissic dome at Isua, has been partially overprinted by a 1,575 Ma metamorphic event, and local indications of the overprint have been preserved in the recrystallized dyke.

The isotopic data obtained on the Proterozoic dyke presents a similar history. Scatter of both Pb and Sr isotopes is attributed to assimilation of varying amounts of pre-existing crustal material. If an upper limit for the age of emplacement of the dyke is taken to be pre-Qorqut (approximately 2,600 Ma) the Pb data are consistent with assimilation of 5 to 15 percent of older, less radiogenic lead from the host rocks. Obvious deuteric alteration of the constituent mineralogy (Plates 7-10) serves as the mechanism by which variation in the Sr data is produced. Several samples of Dyke III display markedly low Pb and Sr isotopic ratios (also Rb and Sr concentrations). During emplacement of the magma, it is possible that portions of the wall rock were rafted off into the ascending magma and completely assimilated on a local scale prior to final crystallization of the melt. The two samples in question here lie on a lead growth line of approximately 2,600 Ma, generated from older, less radiogenic lead. However, this data is not sufficient to warrant formulation of an entire model for emplacement and

subsequent contamination of the primary magma.

Studies have been conducted dealing with the re-mobilization of Rb and Sr on mineral systems under metamorphic conditions (Baadsgaard and van Breemen, 1970; Kesmarky, 1977; Banks, 1980). Micaceous minerals are shown to be the most susceptible to the migration of Rb and Sr plus other alkali elements. If the whole rock system is to be isotopically disturbed, the range of migration of these elements is important. Results from the studies have shown limited mobility, however other studies (Hoffman, 1971; Brooks, 1980) have demonstrated the partial open system behaviour of whole rock suites. Complete resetting of the whole rock system during metamorphism has been demonstrated by Taylor (1975) and Weber *et al.* (1975).

B. Conclusions

It has been shown that Rb, Sr and Pb contents of dolerite dykes show element variations that reflect the nature of the environment intruded, and therefore are not representative of the composition of the primary magma. Observed variations in the ratios of $^{87}\text{Sr}/^{86}\text{Sr}$ to $^{87}\text{Rb}/^{86}\text{Sr}$ reflect contamination of the primary magma by assimilation of wall rock, later limited migration of alkalis including Rb and possible overprinting caused by metamorphism of gneisses surrounding the study area approximately 1,575 Ma ago. Pb results are entirely consistent with the crustal contamination model, but yield no evidence for metamorphism having occurred at 1,575 Ma.

All data presented coincide with crustal contamination models brought forth for rocks of the Archaean Gneissic Complex of Greenland (Taylor *et al.*, 1980; Moorbath *et al.*, 1981).

The data obtained present an argument for assimilation of older crust. The very nature of the results dictate directions in which follow-up research may be oriented. Further isotopic investigations, perhaps U-Th-Pb and Sm-Nd are clearly required, in addition to further trace and rare-earth element geochemical investigations. By obtaining a more complete understanding of the nature and absolute degree of alteration and contamination of the primary magma, it may then be possible to formulate models based on isotopic research, which lead to corroboration of the age(s) of emplacement for the Ameralik dykes and further definition of their metamorphic history.

Based on results obtained during this study, several conclusions regarding the origin and history of the Ameralik dykes are given:

- 1) The Pb-Pb results indicate the Ameralik dykes as represented by Dykes I and II are approximately $3,197 \pm 45$ Ma old and possibly represent a minor magmatic event preceding emplacement of the Nuk gneiss protoliths.
- 2) Wide variability in Rb-Sr data indicate the dykes have been subjected to possibly multi-episodic metamorphic events which have upset and partially reset certain isotope clocks of the dykes.
- 3) Post-emplacement migration of alkalis and recrystallization of some of the dykes, with the introduction of scapolite, have had variable effect on the isotope systems examined. Pb-Pb is apparently less affected by the chemical and mineralogical changes while Rb-Sr shows a much greater response to the changes. It is suggested here that metamorphism around 1,575 Ma has partially affected the Rb-Sr clock, but the Pb system has remained essentially closed since 3,197 Ma.
- 4) Scatter in the Rb-Sr data is attributed to the following:
 - a) assimilation of up to 15 percent pre-existing crustal material during emplacement.
 - b) local migration of alkalis across the dyke margin (residence contamination) during metamorphism.
 - c) recrystallization of Dyke I with the introduction of scapolite.
- 5) Scatter in the Pb-Pb data is attributed to:
 - a) assimilation of pre-existing crustal material during emplacement
 - b) growth of U-Th bearing epidote group minerals during deuteric alteration.
- 6) The growth curve intercept age of $3,233 \pm 131$ Ma obtained for the "Proterozoic" Dyke III may not be indicative of the true time of emplacement. The MSWD of 71.13 indicates variation in the measured isotopic ratios is outside analytical error and that the scatter in the data is statistically significant. The age of the dyke is within error of those obtained for Dykes I and II and does not preclude the possibility that the dyke is also of the

Ameralik swarm.

7) Dyke III displays variability in isotopic behaviour comparable with that of the Ameralik dykes. Erratic Rb and Sr behaviour is attributed to the combined effects of chemical differentiation during cooling, rafting off and complete digestion of xenoliths of the host rock during emplacement and varying degrees of post-emplacement deuteric alteration.

8) Chemically, Dyke III is distinct from the others studied. Similar Pb-Pb trends suggest the magma has assimilated similar amounts of identical, though older, crustal material.

VII. REFERENCES CITED

- Allaart, J.H., 1976a, Ketilidian mobile belt in Southern Greenland. In: Escher, A. and Watt, W.S. (eds) *Geology of Greenland*, Geological Survey of Greenland, Copenhagen, 121-149.
- Allaart, J.H., 1976b, The Pre-3,760 my old supracrustal rocks of the Isua area, Central West Greenland, and the associated occurrence of quartz banded ironstone. In: Windley, B.F. (ed) *The Early History of the Earth*, 177-189.
- Baadsgaard, H., 1973, U-Th-Pb dates on zircons from the early Precambrian Amitsoq gneiss, Godthaab District, West Greenland, *Earth Pl. Sci. Lett.*, 19, 22-28.
- Baadsgaard, H., 1976, Further U-Pb Dates on zircons from the early Precambrian rocks of the Godthaabsfjord Area, West Greenland. *Earth Planet. Sci. Lett.*, 33, 261-267.
- Baadsgaard, H. and McGregor, V.R., 1981, The U-Th-Pb systematics of zircons from the type Nuk gneisses, Godthaabsfjord, West Greenland. *Geochim. Cosmochim. Acta* 45, 1099-1109.
- Baadsgaard, H., Lambert, R. St. J. and Krupicka, J., 1976, Mineral isotopic age relationships in the polymetamorphic Amitsoq gneisses, Godthaab District, West Greenland, *Geochim. Cosmochim. Acta*, 40, 513-527.
- Banks, C.S., 1980, *Geochronology, general geology and structure of Hill Island-Tazin Lake areas*. Unpublished M.Sc. Thesis, University of Alberta.
- Black, L.P., Gale, N.H., Moorbath, S., Pankhurst, R.J. and McGregor, V.R., 1971, Isotopic dating of very early Precambrian amphibolite facies gneisses from the Godthaab District, West Greenland, *Earth Pl. Sci. Lett.*, 12, 245-259.
- Black L.P., Moorbath, S., Pankhurst, R.J. and Windley, B.F., 1973, $^{207}\text{Pb}/^{206}\text{Pb}$ whole rock age of the Archaean granulite facies metamorphic event in West Greenland, *Nature Phys. Sci.*, 244, 50-53.
- Boak, J.L. and Dymek, R.F., 1982, Metamorphism of the ca. 3,800 Ma supracrustal rocks at Isua, West Greenland: implications for early Archaean crustal evolution, *Earth Planet. Sci.*, 59, 155-176.
- Bridgwater, D. and McGregor, V.R., 1974a, Field mapping of the very early Precambrian rocks of the Godthaabsfjord region, southern West Greenland, *Rapp. Gronlands Geol. Unders.*, 65, 39-44.
- Bridgwater, D. and McGregor, V.R., 1974b, Field work on the very early Precambrian rocks of the Isua area, southern West Greenland, *Rapp. Gronlands Geol. Unders.*, 65, 49-54.
- Bridgwater, D., Keto, L., McGregor, V.R. and Myers, J.S., 1976, Archaean gneiss complex

- of Greenland. In: Escher, A. and Watt, W.S. (eds) *Geology of Greenland*, Geological Survey of Greenland, Copenhagen, 19-76.
- Bridgwater, D., McGregor, V.R. and Myers, J.S., 1974, A horizontal tectonic regime in the early Archaean of Greenland and its implications for early crustal thickening. *Precambrian Research*, 1, 179-197.
- Bridgwater, D. *et al.*, 1979, International field work on Archaean gneisses in the Godthaabsfjord-Isua area, West Greenland, *Rapp. Gronlands Geol. Unders.*, 95, 66-71.
- Brooks, C., 1980, Aphebian overprinting in the Superior Province, east of James Bay, *Can. J. Earth Sci.*, 17, 526-532.
- Chadwick, B. and Coe, K., 1976, New evidence relating to Archaean events in southern West Greenland. In: Windley, B.F. (ed) *The Early History of the Earth*, 203-211.
- Chaplin, C.E., 1981, Isotope geology of the Gloserheia Granite Pegmatite. Unpublished M Sc. Thesis, University of Alberta.
- Cumming, G.L. and Richards, J.R., 1975, Ore lead isotope ratios in a continuously changing Earth. *Earth Planet. Sci. Lett.*, 28, 155-171.
- Davis, D.W., 1978, Determination of the ^{87}Rb decay constant. An Rb/Sr and Pb/Pb study of the Labrador Archaean complex. Unpublished Ph D. thesis, University of Alberta.
- Deer, W.A., Howie, R.A. and Zussman, J., 1966, *An Introduction to the Rock-Forming Minerals*, Longman, London.
- Dickin, A.P., 1981, Isotope geochemistry of Tertiary igneous rocks from the Isle of Skye, N.W. Scotland, *J. Petrol.*, 22, 155-189.
- Dostal, J. and Fratta, M., 1977, Trace element geochemistry of a Precambrian diabase dyke from Western Ontario. *Can. J. Earth Sci.*, 14, 2941-2944.
- Escher, A., Sorensen, K. and Zeck, H.P., 1976, Nagssugtoqidian mobile belt in West Greenland. In: Escher, A. and Watt, W.S. (eds) *Geology of Greenland*, Geological Survey of Greenland, Copenhagen, 77-95.
- Fisher, G.W. and Lasaga, A.C., 1981, Irreversible thermodynamics in Petrology. In: Ribbe, P.H. (ed) *Kinetics of Geochemical Processes*, Min. Soc. Am. Reviews in Mineralogy, vol. 8, 171-208.
- Fratta, M. and Shaw, D.M., 1974, 'Residence' contamination of K, Rb, Li and Tl in diabase dykes, *Can. J. Earth Sci.*, 11, 422-429.
- Gates, T.M., 1971, Improved dating of Canadian Precambrian dikes and a revised polar wandering curve. Unpublished Ph D. Thesis, Massachusetts Institute of

Technology.

- Gill, R.C.O. and Bridgwater, D., 1976, The Aeralik Dykes of West Greenland, the earliest known basaltic rocks intruding stable continental crust. *Earth Planet. Sci. Lett.*, 29, 276-282.
- Gill, R.C.O. and Bridgwater, D., 1979, Early Archaean basic magmatism in West Greenland: The geochemistry of the Aeralik Dykes. *J. Petrol.* 20, 695-726.
- Hofmann, A.W., 1971, Effect of regional metamorphism on radiometric ages in pelitic rocks. *Carn. Inst. Washington Yearbook*, 70, 242-245.
- Holmes, A., 1946, An estimate of the age of the Earth, *Nature*, 157, 680-684.
- Houtermans, F.G., 1946, Die Isotopenhäufigkeiten im natürlichen Blei und das Alter des Urans., *Naturwissenschaften*, 33, 185-186, 219.
- Jaffey, A.H., Flynn, K.F., Glendenin, L.E., Bentley, W.C. and Essling, A.M., 1971, Precision measurements of the half lives and specific activities of ^{235}U and ^{238}U . *Phys. Rev. C4*, 1889-1906.
- Kesmarky, S., 1977, Rates of migration of alkalis and strontium ions in heated quartz monzonite, Unpublished M Sc. thesis, University of Alberta.
- Krstic, D., 1981, Geochronology of the Charlebois Lake area, Northeastern Saskatchewan, Unpublished M Sc. thesis, University of Alberta.
- Lambert, R. St J. and Holland, J.G., 1976, Amitsoq gneiss geochemistry; preliminary observations. In: Windley, B.F. (ed) *The Early History of the Earth*, 191-201.
- McGregor, V.R., 1968, Field evidence of very old Precambrian rocks in the Godthaab area, *Rapp. Gronlands Geol. Unders.*, 15, 31-35.
- McGregor, V.R., 1969, Early Precambrian geology of the Godthaab area, *Rapp. Gronlands Geol. Unders.*, 19, 28-30.
- McGregor, V.R., 1973, The early Precambrian gneisses of the Godthab district, West Greenland. *Phil. Trans. R. Soc. Lond. A*, 273, 343-358.
- McGregor, V.R., 1979, Archaean gray gneisses and the origin of the continental crust, Evidence from the Godthaab region, West Greenland. In: Barker, F. (ed) *Trondhjemites, Dacites and Related Rocks*, Elsevier, Amsterdam, 168-204.
- McGregor, V.R. and Bridgwater, D., 1973, Field mapping of Precambrian basement in the Godthaabsfjord area, southern West Greenland, *Rapp. Gronlands Geol. Unders.*, 55, 29-32.
- McGregor, V.R. and Mason, B., 1977, Petrogenesis and geochemistry of metabasaltic

- enclaves in the Amitsoq gneisses, West Greenland. *Am. Mineral.* 62, 887-904.
- Michard-Vitrac, A., Lancelot, J., Allegre, C.J. and Moorbath, S., 1977, U-Pb ages on zircons from early Precambrian rocks of West Greenland and the Minnesota River Valley, *Earth Pl. Sci. Lett.*, 35, 449-453.
- Moorbath, S., 1975. Evolution of Precambrian crust from strontium isotopic evidence. *Nature*, 254, 395-398.
- Moorbath, S., Allaart, J.H., Bridgwater, D. and McGregor, V.R., 1977, Rb-Sr ages of early Archaean supracrustal rocks and Amitsoq gneisses at Isua, *Nature*, 270, 43-45.
- Moorbath, S. and Bell, J.D., 1965. Strontium isotope abundance studies and rubidium-strontium age determinations from the Isle of Skye North-West Scotland. *J. Petrol.* 6, 37-66.
- Moorbath, S., O'Nions, R.K. and Pankhurst, R.J., 1973, Early Archaean age for the Isua Iron Formation, West Greenland, *Nature, Lond.*, 245, 138-139. p 121.
- Moorbath, S., O'Nions, R.K., Pankhurst, R.J., Gale, N.H. and McGregor, V.R., 1972, Further rubidium-strontium age determinations on the very early Precambrian rocks of the Godthaab District, West Greenland. *Nature Phys. Sci.* 240, 78-82.
- Moorbath, S. and Pankhurst, R.J., 1976, Further rubidium-strontium age and isotope evidence for the nature of the late Archaean plutonic event in West Greenland. *Nature*, 262, 124-126.
- Moorbath, S., Taylor, P.N. and Goodwin, R., 1981, Origin of granitic magma by crustal remobilisation: Rb-Sr and Pb/Pb geochronology and isotope geochemistry of the late Archaean Qorqut Granite Complex of southern West Greenland. *Geochim. Cosmochim. Acta* 45, 1051-1060.
- Moorbath, S. and Thompson, R.N., 1980. Strontium isotope geochemistry and petrogenesis of the early Tertiary lava pile of the Isle of Skye, Scotland, and other basic rocks of the British Tertiary Province: and example of magma-crust interaction, *J. Petrol.*, 21, 295-321.
- Moorbath, S. and Welke, H., 1969, Lead isotope studies of igneous rocks from the Isle of Skye, Northwest Scotland. *Earth Planet. Sci. Lett.*, 5, 217-230.
- Myers, J.S., 1976, The early Precambrian gneiss complex of Greenland. In: Windley, B.F. (ed) *The Early History of the Earth*, 165-176.
- Nutman, A., Bridgwater, D., Dimroth, E., Gill, R.C.O. and Rosing, M., 1982, Field work on the early (3,700 Ma) Archaean rocks of the Isua supracrustal belt and adjacent gneisses. *Rapp. Gronlands Geol. Unders.* (in press).
- Patchett, P.J., 1980, Thermal effects of basalt on continental and crustal contamination of magma. *Nature*, 283, 559-561.

- Patchett, P.J., van Breemen, O. and Martin, R.F., 1979, Strontium isotopes and the structural state of feldspars as indicators of post magmatic hydrothermal activity in continental dolerites. *Contrib. Mineral. and Petrol.*, 69, 65-73.
- Pankhurst, R.J. and O'Nions, R.K., 1973, Determination of Rb/Sr and $^{87}\text{Sr}/^{86}\text{Sr}$ ratios of some standard rocks and evaluation of X-Ray Fluorescence Spectrometry in Rb-Sr geochemistry. *Chem. Geol.* 12, 127-136.
- Pankhurst, R.J., Moorbath, S. and McGregor, V.R., 1973a, Late event in the geological evolution of the Godthaab District, West Greenland, *Nature Phys. Sci.*, 243, 24-26.
- Pankhurst, R.J., Moorbath, S., Rex, D.C. and Turner, G., 1973b, Mineral age patterns in ca. 3,700 My old rocks from West Greenland, *Earth Pl. Sci. Lett.*, 20, 157-170.
- Shaw, D.M., 1960a, The Geochemistry of Scapolite. Part I. Previous work and general mineralogy, *J. Petrol.* 1, 218-260.
- Shaw, D.M., 1960b, The Geochemistry of Scapolite. Part II. Trace elements, petrology and general geochemistry, *J. Petrol.* 1, 261-285.
- Stacey, J.S. and Kramers, J.D., 1975, Approximation of terrestrial lead isotope evolution by a two-stage model. *Earth Planet. Sci. Lett.*, 26, 207-221.
- Tatsumoto, M., Knight, R.J. and Allegre, C.J., 1973, Time differences in the formation of meteorites as determined from the ratio of ^{207}Pb to ^{206}Pb , *Science*, 180, 1279-1283.
- Taylor, P.N., Moorbath, S., Goodwin, R. and Petrykowski, A., 1980, Crustal contamination as an indicator of the extent of the early Archaean crust: Pb isotopic evidence from the late Archaean gneisses of West Greenland. *Geochim. Cosmochim. Acta* 44, 1437-1453.
- Thompson, R.N., 1982, Magmatism of the British Tertiary Volcanic Province, *Scot. J. Geol.*, 18, 49-107.
- Weber, W., Anderson, R.K. and Clark, G.S., 1975, Geology and geochronology of the Wollaston Lake fold belt in northern Manitoba, *Can. J. Earth Sci.*, 12, 1749-1759.
- Wells, P.R.A., 1976, Late Archaean metamorphism in the Buksefjorden region, southern West Greenland, *Contrib. Mineral. Petrol.*, 56, 229-242.

VIII. APPENDIX I

Table 2. Rb/Sr Isotope Results, Isua Dykes

<u>Sample Number</u>	<u>$^{87}\text{Sr}/^{86}\text{Sr}$</u>	<u>$^{87}\text{Rb}/^{86}\text{Sr}$</u>	<u>Rb ppm</u>	<u>Sr ppm</u>
117947	0.70727	0.1391	4.60	95.74
158401	0.70626	0.1133	3.03	77.27
158440	0.70958	0.0797	1.30	51.46
171754	0.71509	0.0690	2.92	122.68
171761	0.70826	0.1233	3.54	83.11
173232	0.85692	4.0766	98.82	71.15
173235	0.70901	0.1280	4.19	94.71
173237	0.72680	0.4928	16.22	95.44
173238	0.70546	0.0657	2.19	96.50
173277	0.71013	0.0214	0.92	123.97
248209	0.71254	0.0471	1.06	65.02
248210	0.70867	0.0736	1.99	78.02
248222	0.70678	0.1318	3.67	80.52
248223	0.70928	0.1697	5.19	88.46
248224	0.70680	0.1347	3.59	76.98
248225	0.70391	0.0556	1.71	89.11
248230	0.72343	0.3158	10.99	100.85
248232	0.72193	0.1863	6.24	97.05
248233	0.70496	0.0869	2.31	76.74
248239	0.80030	2.4594	78.82	93.56
248243	0.71215	0.2212	5.18	67.74
248253	0.71359	0.3454	8.60	72.24
248253*	0.71329	0.3405	8.62	73.10
248255	0.70926	0.1889	5.04	77.14
248256	0.70589	0.0759	2.04	77.73
248257	0.70431	0.0724	2.13	85.00

Table 2 cont.

<u>Sample Number</u>	$^{87}\text{Sr}/^{86}\text{Sr}$	$^{87}\text{Rb}/^{86}\text{Sr}$	<u>Rb ppm</u>	<u>Sr ppm</u>
248260	0.70633	0.1107	3.21	83.74
248261	0.71230	0.0958	2.49	75.21
225901A	0.75802	0.9952	53.68	156.80
225901B	0.73323	0.3913	21.03	146.64
225901C	0.75040	0.8712	44.26	147.59
225901D	0.72129	0.2107	7.28	100.16
225901E	0.71236	0.1294	3.61	80.75
225952A	0.70763	0.1120	2.29	59.19
225952B	0.70911	0.1683	4.99	86.91
225952C	0.70935	0.1847	5.28	82.66
225952D	0.70875	0.1459	4.45	88.25
225952E	0.70953	0.1800	5.15	82.72
225952F	0.71453	0.4103	16.90	119.24
292229A	0.70350	0.0738	2.03	79.49
292229B	0.70474	0.0888	2.16	70.26
292229C	0.70439	0.0888	2.30	74.89
292229D	0.70307	0.0512	1.41	79.39
292229E	0.70342	0.0600	1.65	79.51
292229F+	0.70531	0.1082	2.83	76.58
292229G	0.70512	0.1089	2.81	74.71
292229H	0.70308	0.0636	1.66	75.37
292229I	0.70278	0.0749	1.83	70.72
292229J	0.70485	0.1050	2.68	73.86
292229K	0.70495	0.1131	2.99	76.49
292229L	0.71803	0.2346	6.15	75.92
292229M	0.70421	0.0753	1.98	75.91
292229N	0.70534	0.1088	2.47	65.72
292229O	0.70659	0.1261	3.08	70.63

Table 2 cont.

<u>Sample Number</u>	<u>$^{87}\text{Sr}/^{86}\text{Sr}$</u>	<u>$^{87}\text{Rb}/^{86}\text{Sr}$</u>	<u>Rb ppm</u>	<u>Sr ppm</u>
292229P	0.70664	0.1282	3.51	79.13
292229Q	0.70524	0.1015	2.54	72.26
292229R	0.72737	2.8718	10.15	84.12
292229S	0.90779	4.0925	105.27	75.87
292229T	0.70796	0.1294	3.46	77.02
292229U	0.71252	0.1839	5.85	92.08
292229V	0.72655	0.4049	7.54	54.00
292229W	0.73482	0.8102	14.50	51.91
292229X	0.71163	0.0651	1.82	80.84
292229Y	0.70630	0.1118	2.84	73.51
292229Z	0.71497	0.1818	7.35	75.19
292229AB	0.72049	0.2158	5.85	78.46
292229AC	0.70673	0.1079	3.04	81.47
292229AD	0.70938	0.1615	3.76	67.36
292229AE	0.73210	0.4784	7.84	47.53
292234A	0.74843	1.2133	2.96	709
292234B	0.70773	0.1236	3.81	89.21
292234C	0.70709	0.1085	3.97	105.87
292234D	0.70845	0.1556	4.95	91.97
292234E	0.70857	0.1575	4.56	83.82
292234F	0.70699	0.1092	3.70	97.92
292234G	0.70713	0.1213	3.96	94.49
292234H	0.70751	0.1281	3.92	88.54
292234I	0.70886	0.1802	5.09	81.85
292234J	0.70936	0.1860	5.13	73.73
292234L	0.70814	0.1546	4.73	86.91
292234N	0.70822	0.1336	4.10	88.72
292234O	0.70835	0.1145	3.81	96.28

Table 2 cont.

<u>Sample Number</u>	<u>$^{87}\text{Sr}/^{86}\text{Sr}$</u>	<u>$^{87}\text{Rb}/^{86}\text{Sr}$</u>	<u>Rb ppm</u>	<u>Sr ppm</u>
292234P	0.71118	0.0817	1.58	53.26

* Duplicate sample

+ 292229F values averaged from duplicate analyses giving results:

$$^{87}\text{Sr}/^{86}\text{Sr} = 0.70542 \pm 0.00005, 0.70521 \pm 0.00003$$

$$^{87}\text{Sr}/^{87}\text{Rb} = 0.1079 \pm 0.0002, 0.1084 \pm 0.0001$$

$$\text{Rb ppm} = 2.78 \pm 0.02, 2.88 \pm 0.03$$

$$\text{Sr ppm} = 76.52 \pm 0.01, 76.64 \pm 0.01$$

Table 3

Corrected Pb/Pb Isotope Results, Isua Dykes

<u>Sample Number</u>	<u>$^{206}\text{Pb}/^{204}\text{Pb}$</u>	<u>$^{207}\text{Pb}/^{204}\text{Pb}$</u>	<u>$^{208}\text{Pb}/^{204}\text{Pb}$</u>
248222	16.540	14.795	36.292
248223	13.026	13.932	32.897
248255	13.415	14.223	32.840
248257	13.510	14.313	32.598
248260	15.168	14.412	33.545
248221	12.760	14.008	31.929
248233	13.066	14.231	32.075
248229	12.608	13.971	32.146
248230	13.484	14.290	32.478
248252	13.292	14.288	32.267
248239	12.611	13.684	31.440
248243	12.927	13.865	32.709
248256	13.364	14.239	32.981
248259	13.589	14.153	32.870
248261	13.363	14.194	32.196
225952A	19.094	15.584	39.562
225952B	14.711	14.658	35.108
225952C	13.842	14.381	34.029
225952D	14.959	14.661	35.473
225952E	14.431	14.536	34.716
225952F	15.240	14.735	37.431
171754	13.389	14.031	33.250
173277	13.184	13.899	32.931
248109	12.167	13.576	32.052
248210	12.016	13.511	31.989
248232	14.628	14.762	32.729

Table 3 cont.

<u>Sample Number</u>	<u>$^{206}\text{Pb}/^{204}\text{Pb}$</u>	<u>$^{207}\text{Pb}/^{204}\text{Pb}$</u>	<u>$^{208}\text{Pb}/^{204}\text{Pb}$</u>
158440	19.351	15.636	39.009*
158401	13.289	14.259	32.740
171761	16.726	15.462	36.530
248107	12.651	13.942	32.600
248224	14.856	14.633	34.410
248225	19.451	16.091	42.340
292234A	22.840	16.264	47.836
292234B	14.906	14.508	35.890
292234C	14.204	14.379	34.571
292234D	14.014	14.289	34.426
292234E	14.005	14.258	34.380
292234F	14.129	14.355	34.725
292234G	14.283	14.380	35.241
292234H	14.444	14.443	35.205
292234I	14.421	14.387	34.823
292234J	14.266	14.369	34.788
292234K	14.307	14.389	34.833
292234L	14.152	14.321	34.481
292234N	15.027	14.590	35.456
292234O	14.360	14.406	34.927
292234P	22.403	16.139	44.555
292229A	13.150	14.186	32.491
292229B	12.745	14.057	32.018
292229C	12.785	14.062	31.996
292229D	12.705	14.030	32.085
292229E	12.819	14.122	32.206
292229F	12.753	14.060	32.022
292229G	12.952	14.120	32.189

Table 3 cont

<u>Sample Number</u>	<u>$^{206}\text{Pb}/^{204}\text{Pb}$</u>	<u>$^{207}\text{Pb}/^{204}\text{Pb}$</u>	<u>$^{208}\text{Pb}/^{204}\text{Pb}$</u>
292229H	13.609	14.349	33.007
292229I	13.962	14.547	33.379
292229J	12.745	14.071	31.981
292229K	12.783	14.070	32.040
292229L	12.825	14.093	31.880
292229M	12.868	14.121	32.086
292229N	12.719	14.029	31.965
292229O	12.756	14.057	32.020
292229P	12.990	14.185	32.075
292229Q	12.504	13.905	32.127
292229R	17.435	15.935	33.935
292229S	14.341	14.809	32.168
292229T	12.037	14.103	31.902
292229U	12.814	14.067	32.168
292229V	12.469	13.887	32.083
292229X	12.464	13.885	32.133
292229Y	12.609	13.976	32.506
292229Z	12.488	13.891	32.250
292229AA	12.470	13.888	32.267
292229AB	12.432	13.879	32.200
292229AC	12.465	13.865	32.233
292229AD	12.532	13.888	32.300
292229AE	12.667	13.945	32.291
292229A*	13.107	14.179	32.291
292229B*	12.750	14.074	32.051
292229C*	12.781	14.084	32.150
292229D*	12.652	13.997	31.988
292229E*	12.754	14.058	31.977

Table 3 cont.

<u>Sample Number</u>	<u>$^{206}\text{Pb}/^{204}\text{Pb}$</u>	<u>$^{207}\text{Pb}/^{204}\text{Pb}$</u>	<u>$^{208}\text{Pb}/^{204}\text{Pb}$</u>
292229F*	12.751	14.067	32.031

* Duplicate analyses

Table 4

Rb/Sr Isotope Data, Isua Proterozoic Dyke

<u>Sample Number</u>	<u>⁸⁷Sr/⁸⁶Sr</u>	<u>⁸⁷Rb/⁸⁶Sr</u>	<u>Rb ppm</u>	<u>Sr ppm</u>
292289A	0.71623	0.3710	24.44	190.79
292289B	0.70996	0.2081	16.65	231.47
292289C	0.70450	0.0571	1.79	89.97
292289D	0.71604	0.390	30.78	228.46
292289E	0.71850	0.4765	39.77	241.70
292289F	0.71106	0.4229	37.87	259.36
292289G	0.7071	0.2475	21.68	253.51
292289H	0.71474	0.2892	24.16	241.79
292289I	0.71089	0.1811	18.24	291.45
292289J	0.71456	0.4316	33.52	224.82
292289K	0.71393	0.3313	26.30	229.86
292289L	0.72986	0.1390	5.34	111.43
292289M	0.71504	0.3392	28.84	246.13
292289N	0.71202	0.2223	19.99	260.29
292289O	0.71496	0.3213	29.18	262.89
292289P	0.71124	0.2160	20.38	273.08
292289Q	0.71935	0.4566	39.34	249.57
292289R	0.71555	0.3044	26.39	233.65

Table 5

Corrected Pb/Pb Isotope Results, Isua Proterozoic Dyke

<u>Sample Number</u>	<u>$^{206}\text{Pb}/^{204}\text{Pb}$</u>	<u>$^{207}\text{Pb}/^{204}\text{Pb}$</u>	<u>$^{208}\text{Pb}/^{204}\text{Pb}$</u>
292289B	14.327	14.524	34.742
292289C	13.076	13.943	33.128
292289D	15.736	14.991	36.686
292289E	15.417	14.689	36.337
292289F	14.661	14.534	35.356
292289G	15.903	14.955	36.775
292289H	13.845	14.352	34.016
292289I	14.839	14.655	35.324
292289J	15.929	15.051	36.769
292289K	16.068	14.987	37.238
292289L	12.646	13.878	32.569
292289M	15.341	14.798	36.023
292289N	15.643	14.993	36.476
292289O	14.409	14.540	34.836
292289P	15.536	14.907	36.190
292289Q	14.518	14.611	35.031
292289R	14.364	14.581	34.551

IX. APPENDIX II

A. Rb-Sr Analytical Procedures

During the course of this project, all samples were directly prepared from hand specimen. To minimize any possible surface alteration effects on the whole rock isotopic composition, each sample was completely skinned by removing the entire outer surface with a high speed 6 inch, water cooled diamond saw. The rocks in turn were washed with 1x distilled water to lessen any possible contamination by surface adsorption during cutting. Following cutting the rocks were reduced to pebble size with a jaw crusher, and finally reduced to powder in a TEMA swing mill.

Rb and Sr concentrations were determined by X-Ray Fluorescence Spectrometry utilizing the methods described by Pankhurst and O'Nions (1973). Samples were then weighed out such that approximately 20 μg total Sr would be present and then spiked with an equal aliquot of a mixed Rb/Sr spike (4.2268 $\mu\text{g}/\text{ml}$ Rb, 2.00295 $\mu\text{g}/\text{ml}$ Sr). All spikes used in this study were calibrated by Dr. H. Baadsgaard.

Decomposition and equilibration of sample and spike were achieved by overnight subboiling refluxing in a mixture of 10 ml. concentrated HF and 5 ml. concentrated HNO_3 . The samples were evaporated to dryness, moistened with several drops 3x distilled H_2O and redissolved in 5 ml. HNO_3 , in order that residual fluorides were converted to nitrates. This step was completed twice to ensure complete fluoride conversion. Final sample equilibration was obtained by adding 15 ml. 3x distilled H_2O and 5 ml. HNO_3 to the residue and evaporating the solution down until an approximately 1:1 acid to water mixture remained. This solution was decanted into a 15 ml. teflon test tube and centrifuged to remove any residue remaining. The supernate was transferred to a 15 ml. silica centrifuge tube to which 5 drops of a supersaturated $\text{Ba}(\text{NO}_3)_2$ solution had been added. In most cases gentle agitation of the test tube produced precipitation of $(\text{Ba,Sr})(\text{NO}_3)_2$. In cases where no precipitate was evident, it could be induced by gently rubbing the test tube walls with a teflon rod and adding additional HNO_3 . Once precipitation was evident, the test tubes were allowed to stand overnight.

The suspension was then centrifuged and the Rb bearing supernate was transferred into platinum dishes to which 0.5 ml. concentrated H_2SO_4 was added, and the

mixture evaporated on a hotplate. The residual sulphosalts were then ignited to drive off the SO_3 and the Rb was leached from the oxidic ash in a minimum amount of H_2O . This solution could then be directly loaded onto the side filament of an outgassed rhenium double filament. Due to the low concentrations of K in the samples, standard perchlorate co-precipitation of the Rb was not done.

The centrifuge tube containing the $(\text{Ba,Sr})(\text{NO}_3)_2$ precipitate was carefully rinsed out with H_2O , being careful not to disturb the precipitate, which was then allowed to dry. The precipitate was further purified by redissolving in a drop of H_2O , transferring the drop to a 3 ml. silica centrifuge tube and reprecipitating by adding 1-2 ml. HNO_3 . The supernate was discarded and the precipitate allowed to dry once more. The precipitate was dissolved in 0.5 ml. 2.3N HCl and carefully loaded into teflon columns containing 16 centimetres DOWEX 50W-X12 100-200 mesh cation exchange resin. The columns were first equilibrated with 20 ml. 1x distilled HCl, 4 ml. vapour-distilled 6N HCl, 4-8 ml. 3x H_2O and 4 ml. vapour-distilled 2.3N HCl. The column was eluted with vapour-distilled 2.3N HCl and the strontium was collected in the eluted fraction between 7.5 and 11.5 ml.

The eluate was evaporated to dryness and the residue examined. If bladed BaCl_2 crystals were present, the entire column purification procedure was repeated, if not, the Sr was taken up in a drop of vapour-distilled 2.5N HCl and evaporated on the side filament of a rhenium double filament.

Sr sample loads were analyzed utilizing an ALDERMASTON MICROMASS 30 mass spectrometer with an online HP 9825A minicomputer. Individual masses were measured by peak switching between preset electromagnet current positions and recording the digital voltmeter output. All Rb analyses were performed on a homebuilt 12 inch 90° magnet sector solid source mass spectrometer with an online TI 980A minicomputer. Data was collected using a 5.5kv accelerating voltage, peak switching mode and Faraday cup collection system. Reduction of Rb and Sr data was accomplished utilizing computer programmes written by Dr. G.L. Cumming of the Department of Physics.

B. Pb-Pb Analytical Procedures

For the purpose of this study, one gram of finely ground whole rock powder was placed in a teflon beaker to which 10 ml. vapour-distilled HF and 5 ml. vapour distilled HNO_3 were added. In most cases, complete sample decomposition was achieved with one such treatment, if not, a second identical dissolution was made. The solution was evaporated to dryness, the residue moistened with a drop of 3x distilled H_2O and redissolved in 5 ml. HNO_3 . This step was done twice to ensure complete fluoride-nitrate conversion.


After the second evaporation, the residue was dissolved in 4 ml. H_2O and heated for several minutes, at which time 4 ml. HNO_3 was added. This mixture was again heated for several minutes, being allowed to partially evaporate. In this manner a >1:1 HNO_3 to H_2O mixture remained. The solution was centrifuged to remove any residual gelatinous material. The supernate was transferred to a 15 ml. silica centrifuge tube to which 10 drops supersaturated $\text{Ba}(\text{NO}_3)_2$ had been added. If $(\text{Pb},\text{Ba})(\text{NO}_3)_2$ precipitation was not evident after gentle agitation, it could be initiated by gentle rubbing of the centrifuge tube walls. Once flocculation of the precipitate had begun, the centrifuge tube was allowed to stand a minimum of two hours.

The precipitate was centrifuged and gently washed with water without disturbing the precipitate, and then dissolved in a drop of H_2O and transferred to a 3 ml. silica centrifuge tube and reprecipitated by adding HNO_3 . The centrifuge tube was allowed to stand a minimum of another 2 hours. After centrifuging and washing once more, the precipitate was allowed to dry. The teflon columns used for the anion exchange purification of the lead were filled with approximately 1 ml. of BIO-RAD AG 1-X8, 100-200 mesh chloride anion exchange resin and equilibrated with 4 ml. 6N HCl, 4 ml. H_2O and 4 ml. 1.5N HCl.

The sample was dissolved in 0.5 ml. 1.5N HCl, eluted to 2.0 ml. and carefully loaded onto the columns. Ba-Pb separation was achieved by passing an additional 4 ml. 1.5N HCl through the columns, then stripping the lead from the columns in 6 ml. H_2O .

During the latter stage of this study, several centilitres of the $\text{Ba}(\text{NO}_3)_2$ used in the Sr chemistry was electrolyzed for 4 days in a teflon beaker with platinum electrodes to remove any contaminant lead. This procedure facilitated combination of the Pb and Sr

chemistry. Sr sample sizes were increased five fold to one gram and spiked with 2 grams mixed Rb/Sr spike. The only change in the chemistry which occurred was that the preliminary eluate from the Pb columns now contained the $(\text{Ba,Sr})\text{Cl}_2$. It was collected and prepared for passage through the H^+ cation exchange columns.

The lead eluate was evaporated to dryness and prepared for analysis in the following manner. First, a drop of silica gel slurry was evaporated on to the rhenium filament, to which the lead, dissolved in a small drop of 2.4N H_3PO_4 , was added. The current being passed through the filament was incrementally increased to 1.5 amperes. When the drop on the filament began to turn amber in colour, the load was gently mixed to ensure complete equilibration of the silica gel and the lead phosphate. At 1.6–1.8 amps, lead phosphosilicate began to precipitate and at 2.0–2.2 amps the remaining H_3PO_4 was fumed off. The filament was briefly brought to 'dull red' to ensure complete evaporation of the phosphoric acid, by raising the filament current to 2.5 amps. The sample was loaded in the ALDERMASTON MICROMASS  source mass spectrometer, and the filament temperature was slowly raised to 1250°C (as measured by optical pyrometer). The beam was allowed to stabilize prior to data acquisition. The mass spectrometer was operated in the peak switching mode with Faraday cup collection system. The accelerating voltage used was 8.7kv (same for Sr). Data collection and reduction was performed using an online HP 9825A minicomputer. The measuring error of the instrument was less than 0.15 per mil (standard error of the weighted mean ratio) as calculated by D. Krstic (1981) from repetitive measurements on an NBS-981 common lead standard.